First Annual Science Day
Faculty of Science-Sohag University
April 20, 2016

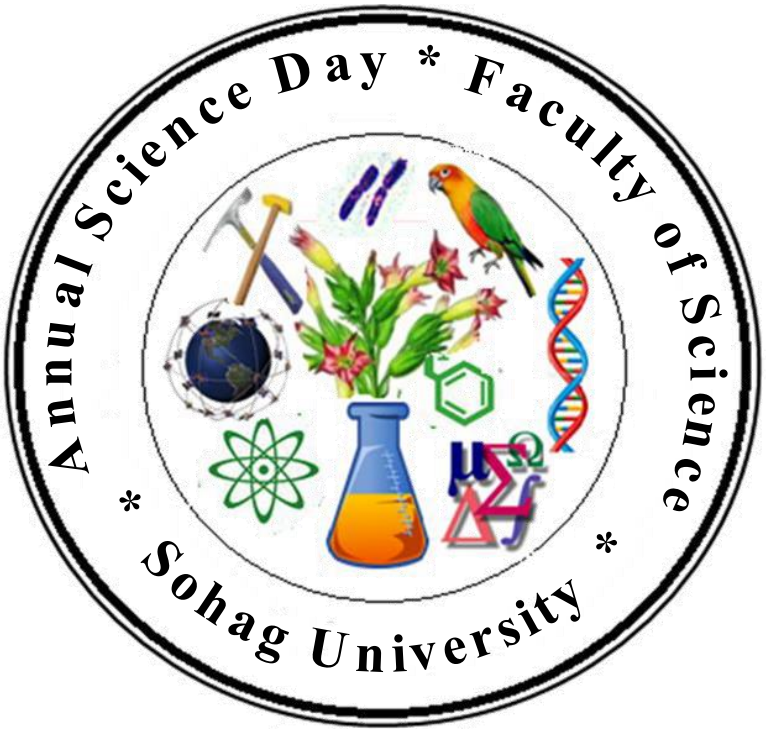

المؤتمر العلمى السنوى الأول لكلية العلوم
جامعة سوهاج

Abstract Book for Papers Published by Staff Members of Faculty of Science during 2015

Contents

Mathematics

Reverse generalized Bessel matrix differential equation, polynomial solutions, and their properties

M. Abul-Dahab, M. Abul-Ez, Z. Kishka and D. Constales
Mathematics Department, Sohag University, Sohag 82524, Egypt

This paper is devoted to the study of reverse generalized Bessel matrix polynomials (RGBMPs) within complex analysis. This study is assumed to be a generalization and improvement of the scalar case into the matrix setting. We give a definition of the reverse generalized Bessel matrix polynomials $\Theta_n(A; B; z), z \in \mathbb{C}$ for parameter (square) matrices A and B, and provide a second-order matrix differential equations satisfied by these polynomials. Subsequently, a Rodrigues-type formula, a matrix recurrence relationship, and a pseudo-generating function are then developed for RGBMPs.

Journal of Mathematical Methods in the Applied Sciences, Volume 38, Issue 6, pages 1005–1013, April 2015, DOI: 10.1002/mma.3020

Locality and classicality: role of entropic inequalities

J. Batle ,M. Abdel-Aty ,C. H. Raymond, Abdalla, Y. Al-hedeethi,
Department of Mathematics, Faculty of Science, Sohag University, 82524, Sohag, Egypt

The use of the so-called entropic inequalities is revisited in the light of new quantum correlation measures, specially nonlocality. We introduce the concept of *classicality* as the nonviolation of these classical inequalities by quantum states of several multiqubit systems and compare it with the nonviolation of Bell inequalities, that is, *locality*. We explore-numerically and analytically-the relationship between several other quantum measures and discover the deep connection existing between them. The results are surprising due to the fact that these measures are very different in their nature and application. The cases for n=2,3,4n=2,3,4 qubits and a generalization to systems with arbitrary number of qubits are studied here when discriminated according to their degree of mixture.

Quantum Information Processing,)5148(646:–6448)5148(47, DOI : /410411:s11128-015-1028-7

Improving the quantum cost of NCT-based reversible circuit

Rasha Montaser, A.Younes, M. Abdel-Aty

Department of Mathematics, Faculty of Science, Sohag University, 82524, Sohag, Egypt

We describe a scalable protocol for optimizing the quantum cost of the 3-bit reversible circuits built using NCT library. This technique takes into account a group theory approach. The algorithm analyzes the equivalent quantum circuits obtained by decomposing the reversible circuit to its elementary quantum gates and then applies optimization rules to reduce the number of the used elementary quantum gates. We apply the obtained algorithm using different quantum cost metrics that compare favorably with the relevant methods.

Quantum Information Processing,)5148(4596–4571)5148(47, **DOI : /410411:s11128-015-0929-9**

Efficient realization of quantum search algorithm using quantum annealing processor with a dissipation

A. H. Homid, A. Abdel-Aty , M. Abdel-Aty , A. Badawi and A.-S. F. Obada
Department of Mathematics, Faculty of Science, Sohag University, 82524, Sohag, Egypt

Following experimental work [Nature , 473, 194 (2011) [CrossRef]], we propose a new physical scheme for perfect implementation of a quantum search algorithm in the presence of qubits dissipation. It is shown that the Grover algorithm is obtained as a special case of the suggested quantum search algorithm. We have generated the quantum gates to realize the required steps for implementing the algorithm. Experimental evidence has been discussed in which, during a critical portion of quantum annealing, the qubits become entangled, and entanglement persists even as these systems reach equilibrium with a thermal environment. Our results provide an encouraging sign that quantum annealing is a viable technology for large-scale quantum computing. It is shown that the protocol can be successfully implemented within the present experimental limits.

***Journal of the Optical Society of America B*, Vol. 32, Issue 9, pp. 2025-2033 (2015), DOI: 10.1364/JOSAB.32.002025**

Analytical Solution of The Two-Qubit Quantum Rabi Model

Doaa A. M. Abo-Kahla, Salah A. Aly, Mahmoud Abdel-Aty

Department of Mathematics, Faculty of Science, Sohag University, 82524, Sohag, Egypt

In this paper, an analytical solution of the two-qubit Rabi model for the general case is presented. Furthermore, a comparison between the information entropies and the Von Neumann entropy (ρA) is given for some special values of the qubit-photon coupling constants in case of the detuning parameters. It is demonstrated that oscillations of the occupation probabilities $\rho 11$,$\rho 22$,$\rho 33$ and $\rho 44$ are equivalent to the case of the spontaneous emission. The occupation probability $\rho 11$ reaches the case of sudden death, when the detuning parameters $\Delta 2$ equals zero.

***International Journal Quantum Information,* DOI : arXiv:1506.01903v3**

Effects of squeezing parameter and time dependent coupling on the evalution of the entanglement between two two-level atoms

S Abdel-Khalek, M Abdel-Aty

In this article we consider the interaction between two two-level atoms and a squeezed field mode. The atom-atom entanglement is discussed by the evolution of the concurrence. von Neumann entropy is used for studying the dynamical behavior of the nonlocal correlation between the squeezed field and two atoms. It is found that the squeeze parameter, atomic motion though the velocity and acceleration parameters play essential roles in the evolution of the atom-atom entanglement and the squeezed field-two atoms nonlocal correlation. The phenomena of the entanglement sudden death and sudden birth is explored.

APPLIED AND COMPUTATIONAL MATHEMATICS 14 (3), 328-335

Information entropy of multi-qubit Rabi system

D. A. M. Abo-Kahla and M. Abdel-Aty

We consider quantum information entropy phenomenon for multi-qubit Rabi system. By introducing different measurements schemes, we establish the relation between information entropy approach and Von Neumann entropy. It is shown that the information entropy is more sensitive to the time development than the Von Neumann entropy. Furthermore, the suggested protocol exhibits excellent scaling of relevant characteristics, with respect to population dynamics, such that more accurate dynamical results may be obtained using information entropy due to variation of the frequency detuning and the coupling constant.

Int. J. Quantum Inform. 13, 1550042 (2015) [10 pages] DOI: 10.1142/S0219749915500422

Multi-Qubit Dynamical Quantum Search Algorithm with Dissipation

A. H. Homid, Mahmoud Abdel-Aty, A.-S. F. Obada

We invoke an efficient search algorithms as a key challenge in multi-qubit quantum systems. An original algorithm called dynamical quantum search algorithm from which Grover algorithm is obtained at a specified time is presented. This algorithm is distinguished by accuracy in obtaining high probability of finding any marked state in a shorter time than Grover algorithm time. The algorithm performance can be improved with respect to the different values of the controlled phase. A new technique is used to generate the dynamical quantum gates in the presence of dissipation effect that helps in implementing the current algorithmm.

arXiv preprint arXiv:1509.04858

New Designs of Universal Reversible Gate Library

R Montaser, A Younes, M Abdel-Aty

We present new algorithms to synthesize exact universal reversible gate library for various types of gates and costs. We use the powerful algebraic software GAP for implementation and examination of our algorithms and the reversible logic synthesis problems have been reduced to group theory problems. It is shown that minimization of arbitrary cost functions of gates and orders of magnitude are faster than its previously counterparts for reversible logic synthesis. Experimental results show that a significant improvement over the previously proposed synthesis algorithm is obtained compared with the existing approaches to reversible logic synthesis.

arXiv preprint arXiv:1512.08991

An efficient scheme for face detection based on contours and feature skin recognition

Mohamed Heshmat, Moheb Girgis, Walaa M Abd-Elhafiez, Seham Elaw
Mathematics Department, Sohag University, Sohag 82524, Egypt

Human face detection is very useful in many applications such as communications, automatic access control systems, video browsing, security control, verification of credit cards, identifying criminals and so on. This work provides a simple and efficient technique to detect human faces in still images. The new method based on skin color, contour drawing and feature extraction. The features under consideration are eyes, nose and mouth. The technique used to extract facial features developed based on feature location with respect to face dimensions. The proposed algorithm was tested on various images and its performance was found to be good in most cases. Experimental results show that our method of human face detection achieves very encouraging results with good accuracy, great speed and simple computations.

2015 10th International Conference on Computer Engineering & Systems (ICCES), 255 - 260, 23-24 Dec. 2015, DOI: 10.1109/ICCES.2015.7393056

Effect of the time-dependent coupling on a superconducting qubit-field system under decoherence: Entanglement and Wehrl entropy

S. Abdel-Khalek, K. Berrada, H. Eleuch,

Department of Mathematics, Faculty of Science, Sohag University, 82524, Sohag, Egypt

The dynamics of a superconducting (SC) qubit interacting with a field under decoherence with and without time-dependent coupling effect is analyzed. Quantum features like the collapse– revivals for the dynamics of population inversion, sudden birth and sudden death of entanglement, and statistical properties are investigated under the phase damping effect. Analytic results for certain parametric conditions are obtained. We analyze the influence of decoherence on the negativity and Wehrl entropy for different values of the physical parameters. We also explore an interesting relation between the SC-field entanglement and Wehrl entropy behavior during the time evolution. We show that the amount of SC-field entanglement can be enhanced as the field tends to be more classical. The studied model of SC-field system with the time-dependent coupling has high practical importance due to their experimental accessibility which may open new perspectives in different tasks of quantum formation processing.

Annals of Physics 361 (2015) 247–258, DOI : http://dx.doi.org/10.1016/j.aop.2015.06.015

Geometric phase and entanglement of Raman photon pairs in the presence of photonic band gap

K. Berrada, C. H. Raymond Ooi, and S. Abdel-Khalek,
Department of Mathematics, Faculty of Science, Sohag University, 82524, Sohag, Egypt

Robustness of the geometric phase (GP) with respect to different noise effects is a basic condition for an effective quantum computation. Here, we propose a useful quantum system with real physical parameters by studying the GP of a pair of Stokes and anti-Stokes photons, involving Raman emission processes with and without photonic band gap (PBG) effect. We show that the properties of GP are very sensitive to the change of the Rabi frequency and time, exhibiting collapse phenomenon as the time becomes significantly large. The system allows us to obtain a state which remains with zero GP for longer times. This result plays a significant role to enhance the stabilization and control of the system dynamics. Finally, we investigate the nonlocal correlation (entanglement) between the pair photons by taking into account the effect of different parameters. An interesting correlation between the GP and entanglement is observed showing that the PBG stabilizes the fluctuations in the system and makes the entanglement more robust against the change of time and frequency.

Journal Of Applied Physics 117, 124904 (2015), DOI : http://dx.doi.org/10.1063/1.4916333

Quantum Entanglement and Geometric Phase of Two Moving Two-Level Atoms

S. Abdel-Khalek,

Department of Mathematics, Faculty of Science, Sohag University, 82524, Sohag, Egypt

An important kind of interaction between two moving two-level atoms and a field mode, where the coupling parameter is taken to be time-dependent, is presented in this paper. Nonlocal correlations between the atoms and the field have been investigated by means of concurrence and von Neumann entropy in terms of the involved parameters of the system. The results show that the atomic motion plays an essential role in the evolution of system dynamics, its nonlocal correlations and geometric phase. Moreover, an interesting correlation between the entanglement and the geometric phase during the evolution was observed. The presented system can be very useful for generating and maintaining high amount of entanglement by means of controlling the parameters of atomic motion.

Open Systems & Information Dynamics Vol. 22, No. 3 (2015) 1550015, DOI : 10.1142/S1230161215500158

Dynamics of Correlations in the Presences of Intrinsic Decoherence

Nour Zidan,
Department of Mathematics, Faculty of Science, Sohag University, 82524, Sohag, Egypt

The dynamics of a mixed spin system governed by *XXZ* model in additional to an intrinsic decoherence is investigated. The behavior of quantum correlation and the degree of entanglement between the two subsystems is quantified by using measurement-induced disturbance and the negativity, respectively. It is shown that, the phenomena of long-lived entanglement appears for larger values of intrinsic decoherence parameters. The degree of entanglement and quantum correlation depend on the dimensions of subsystems which are pass through the external field and the initial states setting. We show that the negativity for some initial classes is more robust than the measurement-induced disturbance, while for some other initial classes the quantum correlations are more robust than entanglement.

Int J Theor Phys (2016) 55:1274–1284, DOI: 10.1007/s10773-015-2768-y

Fixed Point Theorems for Contractive Mappings of integral type in n-Banach Spaces

R. A. Rashwan[a] and H. A. Hammad[b]

[a]Department of Mathematics, Faculty of Science, Assuit University, Assuit 71516, Egypt
E-mail: rr_rashwan54@yahoo.com
[b]Department of Mathematics, Faculty of Science, Sohag University, Sohag 82524, Egypt
E-mail: h_elmagd89@yahoo.com

In this paper, we present some common fixed point theorems for class of mappings satisfying contractive condition of integral type in n-Banach spaces. Our results are version of some known results.

JP Journal of Fixed Point Theory and Applications, 10 (2015), 1-14, DOI : 10.17654/JPFPTA Apr2015_001_014.

A Unique Common Fixed Point Theorems for Weakly Compatible Mappings Under Contractive Conditions in G-Metric Spaces of Integral Type

R. A. Rashwan[a] and H. A. Hammad[b]

[a]Department of Mathematics, Faculty of Science, Assuit University, Assuit 71516, Egypt
E-mail: rr_rashwan54@yahoo.com
[b]Department of Mathematics, Faculty of Science, Sohag University, Sohag 82524, Egypt
E-mail: h_elmagd89@yahoo.com

In this paper, we prove common fixed point theorems for six weakly compatible mappings satisfying the contractive conditions in the setting of Generalized metric spaces satisfying an integral type and the common (E.A) property. Also we redefine the concept of wilson [1] and common (E.A) property in G-metric spaces. Our results generalizes some well known results in the literature.

[1] W. A. Wilson, On semi-metric spaces, Amer. J. Math. 53 (1931), 361-373.

International Journal Functional Analysis, Operator Theory and Applications, 7 (2015), 57-80, DOI: 10.17654/IJFAOTA Feb2015_057_080.

Estimation of some lifetime parameters of generalized Gompertz distribution under progressively type-II censored data

Essam A. Ahmed,

Department of Mathematics, Faculty of Science, Sohag University, 82524, Sohag, Egypt

In this paper, the estimation of parameters of a three-parameter generalized Gompertz distribution based on progressively type-II right censored sample is studied. These methods include the maximum likelihood estimators (MLEs), and Bayesian estimators. Approximate confidence intervals for the unknown parameters as well as reliability function, hazard function and coefficient of variation are constructed based on the s-normal approximation to the asymptotic distribution of MLEs, and log-transformed MLEs. Furthermore, two bootstrap confidence intervals are proposed. Several Bayesian estimates are obtained against different symmetric and asymmetric loss functions such as squared error, LINEX and general entropy. Based on theses loss functions, under gamma priors distributions, Bayes estimates of the unknown parameters and the corresponding credible intervals are obtained by using the Gibbs within Metropolis–Hasting samplers procedure. Finally, a real data set is analyzed to illustrate the proposed methods.

Applied Mathematical Modelling, Volume 39, Issue 18, 15 September 2015, Pages 5567–5578, DOI: 10.1016/j.apm.2015.01.023

Solution of a Quadratic Non-Linear Oscillator by Elliptic Homotopy Averaging Method

A. M. El-Naggar[1], G. M. Ismail[2]

[1]*Department of Mathematics, Faculty of Science, Benha University, Egypt*

[2]*Department of Mathematics, Faculty of Science, Sohag University, 82524, Sohag, Egypt*

In this paper, the periodic solutions of a strongly quadratic nonlinear oscillator whose motion is described with the generalized Van der Pol equation are studied. A new method based on homotopy and averaging is employed to determine the limit cycle motion. Three types of quadratic nonlinearity are considered: the coefficients of the linear and quadratic terms are positive, the coefficient of the linear term is positive and that of the quadratic term is negative and the opposite case. Comparison with the numerical solutions is also presented, revealing that the present method leads to accurate solutions.

Mathematical Sciences Letters, 4, No. 3, 313-317 (2015), DOI: http://dx.doi.org/10.12785/msl/040315

Analytical Solutions of Strongly Non-linear Problems by the Iteration Perturbation Method

A. M. El-Naggar[1], G. M. Ismail[2]

[1]*Department of Mathematics, Faculty of Science, Benha University, Egypt*

[2]*Department of Mathematics, Faculty of Science, Sohag University, 82524, Sohag, Egypt*

This paper applies modified He's iteration perturbation method to study periodic solutions of strongly nonlinear oscillators. Some examples are given to illustrate the effectiveness and convenience of the method. The results are compared with the numerical solution and the comparison showed a proper accuracy of this method.

Journal of Scientific Research & Reports, 5(4): 285-294, 2015, DOI: 10.9734/JSRR/2015/14364

Analytical Solutions for Free Vibration of Strongly Nonlinear Oscillators

M. Abul-Ez, G. M. Ismail and M. M. El-Moshneb,
Department of Mathematics, Faculty of Science, Sohag University, 82524, Sohag, Egypt

In this paper, a nonlinear free vibration of strongly nonlinear oscillators is studied. To this end, we propose a novel technique using He's frequency-amplitude formulation and He's energy balance method called iteration perturbation procedure. A novel technique called iteration perturbation procedure and variational iteration method are presented to obtain the relationship between amplitude and angular frequency. The obtained results are compared with the numerical solution obtained by using the Runge–Kutta method and shown in graphs indicating the effectiveness and convenience of the analytical approximate solutions. These approaches are very effective and simple and with only one iteration leads to high accuracy of the solutions. It is predicted that those methods can be found wide applications in engineering problems, as indicated in this paper.

Information Sciences Letters, 4, No. 2, 101-105 (2015), DOI : http://dx.doi.org/10.12785/isl/040207


قسم الفيزياء
Physics Department

Physics


قسم الفيزياء
Physics Department

EOS of Neutron Matter and Neutron Star Properties

Kh. S. A. Hassaneen, H. M. Abou-Elsebaa, E. A. Sultan, N. N. Abd Allah
Physics department, Faculty of Science, Sohag University, Sohag, Egypt

The Equation of State (EOS) of pure neutron matter at zero temperature is calculated up to five saturation densities within the Brueckner theory with the inclusion of three-body forces. Three different realistic and accurate two-body forces are considered to evaluate the G-matrix effective interaction for nuclear matter. These models are the chiral N3LO, the CD-Bonn and the Argonne V18, which give quite different EOS. Two types of three-body forces are included to the effective interaction, which might be important at densities several times that of nuclear matter density. Using a microscopic EOS for pure neutron matter, static properties of non-rotating neutron stars such as masses and radii are evaluated. The resulting maximum masses of neutron star using different interactions near 2 MΘ are found to be in reasonable agreement with the measured ones PSR J1614−2230 (with M_{max} = 1.97 ± 0.04 MΘ) and PSR J0348+0432 (with Mmax = 2.01 ± 0.04 MΘ).

Journal of Nuclear and Particle Physics 2015, 5(1): 15-20

Microscopic and bulk properties of symmetric nuclear and pure neutron matter with chiral N^3LO nucleon-nucleon force

Kh.S.A. Hassaneen, H.M. Abou-Elsebaa, E.A.Sultan and N.N. Abd Allah
Physics department, Faculty of Science, Sohag University, Sohag, Egypt.

We have studied the single-particle properties and the equation of state (EOS) of symmetric nuclear and neutron matter within the framework of the Brueckner-Hartree-Fock (BHF) approach extended by including a phenomenological three-body force (3BF). Adding the 3BF to the initial two-body force (2BF) and applying a partial-wave expansion, *G*-matrix calculations are performed in pure neutron matter as well as in symmetric nuclear matter. The 3BF is shown to affect signifi-cantly the nuclear matter EOS at high densities above the normal nuclear matter density and it is necessary for reproducing the empirical saturation property of symmetric nuclear matter in a non-relativistic microscopic framework. The calculations have been done using the charge-dependent chiral nucleon-nucleon interaction at order four N^3LO potential and compared with both the CD-Bonn and Argonne V_{18} potentials plus the three-nucleon Urbana interaction. It is found that the calculations with the N^3LO potential alone for symmetric nuclear matter at high density is strongly over bound in the BHF approximation.

International Journal of Scientific & Engineering Research, 6, (1), 2015

Study of topological morphology and optical properties of SnO_2 thin films deposited by RF sputtering technique

A. Alhuthali, M. M El-Nahass, A. A. Atta, M. M. Abd El-Raheem, Khalid M. Elsabawy, A. M. Hassanien,

Transparent conducting thin films of tin dioxide (SnO_2) were prepared on glass substrates by RF sputtering technique. The as-deposited films were annealed at different temperatures (473, 673 and 823 K) for 3 h in air under normal atmospheric pressure. The film structure was characterized using atomic force microscopy (AFM). The optical properties of the prepared and annealed films were studied using their reflectance and transmittance spectra. The Urbach energy was found to decrease with increasing annealing temperature. The estimated direct optical band gap (Egd) values were found to decrease by annealing temperature. The photoluminescence (PL) spectroscopy measurement of the SnO2 film shows that the band to band emission peak atEgPL=4.18 eV. The dispersion curves of the refractive index of SnO2 thin films were found to obey the single oscillator model .

Journal of luminescence, 158(2015) 165-171

Characterization of N and P-type $(SnO_2)_x(ZnO)_{1-x}$ nanoparticles thin films

H. M. Ali, and A. M. Abdel hakeem
Physics Department, Faculty of Science, 82524 Sohag, Sohag University, Egypt

Electron beam evaporation technique was used to deposit $(SnO_2)_x(ZnO)_{1-x}$ thin films with different concentrations of SnO_2 and ZnO. Optical transmittance (T) and reflectance (R) of the films were measured in the wavelength range 200–2500 nm. It was found that the optical properties of the films strongly affected by the ratio of Sn content. The optical energy gap of direct and indirect transition for the films was determined. Values of energy gap were in the range from 3.35 to 4 eV for direct transition, whereas for indirect transition was in the range from 2.53 to 3.43 eV. The electrical resistivity of the films was measured by means of two contact method. Values of electrical resistivity were in the range between 5.06×10^{-4} to 155 Ω cm depending on the ratio of Sn and Zn ratios. A transformation from N-type to P-type semiconductors was observed.

Eur. Phys. J. Appl. Phys. (2015) 72: 10301

Effect of annealing on properties of decorative zirconium oxynitride thin films

S. H. Mohamed, N. M. A. Hadia, H. M. Ali
Physics Department, Faculty of Science, Sohag University, 82524 Sohag, Egypt

Zirconium oxynitrides are excellent candidates for many technological applications, especially decorative applications. For the use of zirconium oxynitrides as decorative coatings, the thermal stability is of crucial importance. Therefore zirconium oxynitrides, containing both oxygen and nitrogen, were prepared by pulsed d.c. reactive magnetron sputtering at $p_{N_2}/(p_{N_2}+p_{O_2})$ of 0.98. The as-prepared films were annealed in air for 1 h. The full set of annealing was 100, 200, 300, 400, 450, 500 and 550°C. The annealed zirconium oxynitride films exhibited nitrogen loss (oxidation). The nitrogen loss results in a great variance in compositional, electrical and optical properties. The energy dispersive analysis of X-ray and X-ray diffraction were used to examine the compositional and structural properties, respectively. A huge increase in the electrical resistivity was observed upon oxidation. The films annealed at higher temperatures (≥ 450°C) showed insulating behavior with low extinction coefficient (< 1) and reasonable refractive index values. The optical band gap values of the films annealed at 500°C and 550°C are in good agreement with the previously reported values for ZrO_2.

Eur. Phys. J. Appl. Phys. (2015) 69: 30301

WO_3 nanowires for optoelectronic and gas sensing applications

N.M.A. Hadia[1], Mohammed S. Alqahtani[2], S. H. Mohamed[1]
[1]Physics Department, Faculty of Science, Sohag University, 82524 Sohag, Egypt
[2]Department of physics and Astronomy, King Saud University, Riyadh 11451, Saudi Arabia

Nanowires (NWs) of WO_3 were synthesized by thermal evaporation of tungsten for potential applications in light emitting diodes (LEDs) and gas sensing. The products were characterized by X -ray diffraction (XRD), scanning and transmission electron microscopy, spectrophotometer and photoluminescence (PL) measurements. XRD revealed the formation of hexagonal WO_3 single crystal phase. Scanning and transmission electron micrographs analyses showed that the hexagonal WO_3 has nanowires in shape with diameters of 30 - 40 nm and lengths extended to 4ȝm. The calculated optical band gap was 3.26 eV and the Urbach energy was 293 meV. The PL emission revealed two strongest peaks at 365 nm and 421 nm which may have significant potential applications in LEDs. The sensing properties of the obtained WO_3NWs were carried out for NO_2 gas and other harmful gasses. The WO_3 NWs sensors were highly sensitive that can detect NO_2 at the sub-ppm level.

J. Appl. Phys. A, 119, Issue 4 (2015) 1261-1267

Enhanced electro-magnetic properties in $La_{0.7}Sr_{0.3}MnO_3/ZrO_2$ Composites

A M Ahmed, H F Mohamed, A K Diab, Abd El-Mo'ez A Mohamed, A E A Mazen and A M Mohamed

Department of Physics, Faculty of Science, Sohag University, Sohag 82524, Egypt

$(La_{0.7}Sr_{0.3}MnO_3)_{1-x}/(ZrO_2)_x$ (x=0.0 – 0.150, step 0.025) composites have been prepared via solid state reaction process. The X-ray diffraction and scanning electron microscopic observations indicate that there are ZrO_2 grains separated from $La_{0.7}Sr_{0.3}MnO_3$ matrix. It has been found that the inclusion of ZrO_2 content decreases the conductivity, magnetization and metal–semiconductor transition, whereas it increases the low field magnetoresistance. Possible effects of grain boundaries on the low field magnetoresistance have been discussed. The small ZrO_2 grains are trapped between $La_{0.7}Sr_{0.3}MnO_3$ grains may be acting as a barrier for spin-polarized tunneling and enhance the low-field magnetoresistance.

Indian J Phys (June 2015) 89(6):561–570

Enhanced low-*fi*eld magnetoresistance of $La_{0.7}Sr_{0.3}Mn_{1-x}Ni_xO_3$ compounds by annealing process

A. M. Ahmed, M. A. Abedellateef, H. A. Abd El-Ghanny, and Abd El Mo'ez A. Mohamed
Physics Department, Faculty of Science, Sohag University, 82524 Sohag, Egypt

A study of Mn-site substitution by Ni2þ and the effect of annealing time in polycrystalline bulk $La_{0.7}Sr_{0.3}MnO_3$ in composition range ($0 \leq x \leq 0.1$) is presented. This study involves structural, electrical, magnetoresistance, and thermoelectric power (TEP) measurements. X-ray diffraction was used to examine the structure for the as-prepared and annealed samples, and it shows that there is no change in structure with annealing time. Electrical resistivity and magnetoresistance are strongly affected by annealing process, where there is a dramatic increase in resistivity with annealing time and an enhancement in magnetoresistance in different temperature ranges. Moreover, conduction mechanisms above and below transition temperature (T_{ms}) are discussed, since, variable-range hopping and small polaron hopping models are applied above Tms, in addition to some experimental relations below it. In addition, the TEP sign changes from positive to negative with doping and annealing.

Phys. Status Solidi A 212, No. 3, 623–631 (2015)

Structural, magnetic and electronic properties on the Li-doped manganites

A.M.Ahmed [a], G.Papavassiliou [b], H.F.Mohamed [a], E.M.M.Ibrahim [a]
[a] *Physics Department, Faculty of Science, SohagUniversity,82524Sohag,Egypt*
[b] *Institute of Materials Science, NCSR Demokritos, AghiaParaskevi, Greece*

We present results of a comprehensive investigation of the structural, frequency dependent ac susceptibility, dc magnetization, magnetoresistance and thermoelectric power measurementsonpoly- crystalline samples of $La_{1-x}Li_xMnO_3$ (0.05rxr0.30). All samples undergo ferromagnetic to paramagnetic transition and metal to semiconductor transition. A cusp in the zero field-cooled in dc magnetization and a frequency dependent peak in the ac susceptibility reveal the glassy behaviors. The out of phase component of the ac susceptibility shows frequency-dependent peaks below the Curie temperature (indicative of glassy behavior)which have previously been interpreted in terms of freezing of clusters. The grain boundaries play a dominant role in the conduction process. The frame work of the magnon and phonon drag concept analyzed thermoelectric power data at low temperature, while small polaron conduction mechanism explained thermoelectric power data at high temperature. It has been found that the percolation threshold sample is x=0.10, so the author's point of view refers to make spot on this sample in the future works.

Journal of Magnetism and Magnetic Materials 392(2015)27–41

The Effect of Temperature and Oxygen Flow Rate on the Morphology of ZnO Nanostructures

M. A. Awad, A. M. Ahmed and E.M.M. Ibrahim
Physics Department, Faculty of Science, Sohag University, 82524 Sohag, Egypt.

Three different morphologies of ZnO nanostructures were prepared by vapor transport on Au coated silicon substrates. Randomly oriented nanowires (NWs) mixed with few nanoflakes were obtained at furnace temperature of 750 °C and oxygen flow rate of 20 sccm. While thicker, longer and denser NWs were obtained at furnace temperature of 900 °C with the same oxygen flow rate of 20 sccm. Keeping the furnace temperature at 750 °C and lowering the oxygen flow rate to 5 sccm, changed the morphology of the NWs to unspecified features with few NWs in between. Both the growth temperature and the oxygen flow rate have proven to have great influence on stoichiometry. The control of the growth and stoichiometry of ZnO may have an impact in optoelectronic applications.

Int. J. New. Hor. Phys. 2, No. 2, 59-61 (2015).

One step syntheses of S incorporated ZnO nanowires for photocatalysis applications

Madeha Ahmed Awad, Eslam Mohamed Mohamed Ibrahim, and Ahmed Mohamed Ahmed
Physics Department, Faculty of Science, Sohag University, 82524 Sohag, Egypt

S incorporated ZnO nanowires (NWs) were prepared by vapor transport method using ZnS bulk precursor. Effects of S incorporation on the structural, morphological, optical as well as photocatalysis performance of ZnO NWs were studied. EDAX analysis revealed existence of S with low ratio. A deformation of the hexagonal nanowires was observed inasmuch to the S existence. X-ray diffraction analysis asserted the formation of a single phase of ZnO with the emergence of two weak peaks identifier for ZnS. The low value of the optical band gap (3.10 eV) was ascribed to the increase in the level of the valence band maximum induced by the S doping. The capability of S incorporated ZnO as a photocatalyst was tested by the decomposition of methylene blue.

Eur. Phys. J. Appl. Phys. (2015) 72: 30303

Theoretical analysis of ZnO and ZnO based alloys as front electrode in CdS/CdTe solar cells

N. M. A. Hadia and H. A. Mohamed
Physics Department, Faculty of Science, Sohag University, 82524 Sohag, Egypt

ITO has unique properties to be used as front electrode in CdS/CdTe solar cells, however ITO is expensivenot abundant and consequently this type of solar cells is still relatively expensive. This work studies theusing of ZnO and ZnO based alloys such as ZnO:Sn, ZnO:Al and ZnO:In as alternative materials of ITO inorder to develop the efficiency of CdS/CdTe solar cells. Both optical and recombination losses have beentaken into consideration. The calculation of optical losses is carried out based on the multiple reflectionseffect as well as absorption in TCO and CdS layers. Both the front and back surfaces recombination ofthe CdTe layer are used to describe the recombination losses. It was found that ZnO and its alloys areconsidered good alternative materials of ITO that used as a front contact in CdS/CdTe cells. The bestresults were obtained for ZnO:Al, where the calculated short-circuit current density is 22.64 mA/cm2atwidth of depletion layer of 0.11 _m, the optical and recombination losses are about 27% and the CdS/CdTeefficiency is about 17.9%.

Optik - International Journal for Light and Electron Optics, 126(19), 2015 1976–1980.

Characteristics and optical properties of MgO nanowires synthesized by solvothermal method

N. M. A. Hadia and H. A. Mohamed
Physics Department, Faculty of Science, Sohag University, 82524 Sohag, Egypt

Magnesium oxide (MgO) nanowires were synthesized by solvothermal method using magnesium nitrate hexahydrate and sodium hydroxide. Field emission scanning electron microscopy (FE-SEM) and transmission scanning electron microscopy (TEM) measurements indicate that the product consists of a large quantity of nanowires with average diameter of 20 nm and average length of several micrometers. Explorations of X-ray diffraction (XRD), energy dispersive analysis of X-ray (EDAX), fourier transformer infrared spectroscopy (FTIR), selected area electronic diffraction (SAED) and high-resolution transmission electron microscope (HRTEM) indicate that the product is high-quality cubic single-crystalline nanowires. The optical properties of the samples are investigated using UV–visible spectroscopy to study the refractive index and optical dielectric constant. The photoluminescence (PL) measurement suggests that the product has an intensive emission centered at 437 nm, showing that the product has potential application in optical devices. The advantages of our method lie in high yield, the easy availability of the starting materials and allowing their large-scale production at low cost.

Materials Science in Semiconductor Processing 29 (2015) 238-244.

Influence of Post Thermal Annealing Effect on the Optical Properties of SnO_2 Films Prepared by Electron Beam Evaporation Technique

N.M.A. Hadia and H. A. Mohamed
Physics Department, Faculty of Science, Sohag University, 82524 Sohag, Egypt

This work reports on the effect of post thermal annealing on the optical properties of SnO_2 films. The films were deposited using electron beam evaporation technique. The films were annealed in air in the temperature range 200-550 ^oC. It was found that the annealing temperature has a significant effect on the optical properties of these films. The films are transparent in the visible region with average transmission of 83%. A high optical energy-gap of 3.65 eV was achieved at temperature 500 ^oC. Many optical parameters such as: refractive index; extinction coefficient; degree of in homogeneity; dielectric constants; single oscillator energy; dispersion energy; oscillator strength; average oscillator wavelength; static dielectric constant; high frequency dielectric constant; thermal emissivity and optical resistivity were calculated as a function of annealing temperature. Finally, SnO_2 films can be used in transparent heat mirror coatings applications due to their low thermal emissivity at high annealing temperature.

International Journal of Thin Films Science and Technology 4, No. 1 (2015) 1-7.

Properties of TiAlN Coating Deposited by MPIIID on TiN substrates

F. M. El-Hossary, A. M. Abd El-Rahman, M. Raaif and D. A. Ghareeb
Physics Department, Faculty of Science, Sohag University, 82524 Sohag, Egypt

Metal plasma immersion ion implantation and deposition (MPIIID) is employed to produce TiAlN hard coatings on Ti substrate. To improve the load bearing capacity of Ti substrate, nitrogen PIII is used to prepare a bearing TiN layer on Ti base substrate. The MPIIID process is performed using Ti50:Al50 target for different nitrogen/argon gas fractions. The effect of N2/Ar gas ratio on the microstructure, mechanical and tribological properties of TiAlN coatings has been studied. The plastic microhardness of TiAlN increases with increasing the nitrogen gas fraction to reach a maximum value of 30 GPa at 100% N2. The plasticity index and the resistance to plastic deformation increase with increasing the nitrogen gas fraction. The wear volume loss of TiAlN coating deposited on TiN substrate decreases by a factor of 103 in comparison with pure Ti. Moreover, the friction coefficient decreases from nearly 0.8 for Ti to 0.25 for TiAlN coatings. The enhanced mechanical and tribological properties of the coating are correlated to the formation of TiAlN hard phase. This phase has random-oriented microstructure, finer grain size, high oxidation resistance and residual internal stress. Moreover, the TiN interface acts as a barrier for the motion of dislocations.

Applied Physics A, 2015

Tribo-Mechanical and Electrochemical Properties of Plasma Nitriding Titanium

F. M. El-Hossary, N.Z. Negm, A. M. Abd El-Rahman, M. Raaif and A. A. Abd El-Moula

Physics Department, Faculty of Science, Sohag University, 82524-Sohag, Egypt

Titanium nitrides have good tribo-mechanical and biomedical properties. They are employed to harden and protect cutting and sliding surfaces for industrial purpose and as a non-toxic outer-surface for bio-medical applications. In this study, pure titanium was nitrided using rf plasma technique. the microstructural, mechanical, tribological, electrochemical and biomedical properties of nitrided titanium were investigated. The x-ray diffraction demonstrates the formation of İ-Ti2N and the cubic į-TiN phases after plasma nitriding. The microhardness of the nitride samples increases as the plasma-processing power increases up to 1300 HV0.1. That represents approximately 7- folds increment in the microhardness in comparison with the untreated titanium. High nitriding rate of 0.17 ȝm2/s was recorded for the sample that was treated at 650 W. The wear and corrosion resistance are improved after plasma nitriding. Moreover, the friction coefficient is reduced from nearly 0.75 for the untreated titanium to 0.25 for the nitride one. An enhancement in the biocompatibility of the nirided titanium has been achieved. The number of grown mesenchymal stem cells was higher for nitrided substrates compared to that of the untreated titanium. The improved tribo-mechanical and electro chemical performance of the nitrided titanium can be attributed to the formation of super-hard titanium nitrided phases.

Surface & Coatings Technology 276 (2015) 658–667

Properties of Titanium Oxynitride prepared by RF Plasma

F. M. El-Hossary, N.Z. Negm, A. M. Abd El-Rahman, M. Raaif and A. A. Abd Elmula
Physics Department, Faculty of Science, Sohag University, 82524-Sohag, Egypt

Titanium oxynitrides combine the properties of metallic oxides and nitrides. In this presentation, titanium was oxynitrided using inductively coupled RF plasma in a gas mixture containing 80% N_2 and 20% O_2. The effect of plasma-processing power from 350 up to 550 W on microstructure, mechanical, tribological, wettability and electrochemical properties of the oxynitrided titanium was examined using different characterization and testing techniques. The results demonstrated the formation of TiO, TiO_2 rutile phase, TiN_xO_y and Ti_2N as a result of plasma oxynitriding. The microhardness of the oxynitrided layers increases up to 766 HV0.1 as the plasma-processing power increases up to 550 W. The wear and corrosion resistance are improved for oxynitrided titanium in comparison with untreated samples. Moreover, the friction coefficient decreases from nearly 0.75 for the pure titanium to nearly 0.3 for oxynitrided titanium. The obtained data shows an increase of surface energy and wettability of titanium oxynitride as the plasma power increases. The formation of hard oxide and oxynitride phases and the transformation of TiO_2 from anatase to rutile structure at relatively high temperature are the main reasons for the good physical and electrochemical properties of titanium oxynitride.

Advances in Chemical Engineering and Science, 5, (2015) 1-14.

Optimized conditions for the improvement of thin film CdS/CdTe solar cells

H. A. Mohamed
Physics Department, Faculty of Science, Sohag University, 82524-Sohag, Egypt

Efficient thin film CdS/CdTe solar cell performance requires optimum parameters of each layer of this cell and of the barrier structure. Moreover, the effect of optical losses, recombination losses at front and back surface of CdTe and recombination losses in the space-charge region (SCR) must be considered in order to really analyze the role of these parameters on the performance of these cells. This work is focused on studying theoretically the effect of the thickness of the front contact (ITO), thickness of the window layer (CdS), thickness of the absorber layer (CdTe), width of the space-charge region and electron lifetime on the efficiency of CdS/CdTe solar cells. The reflection losses from interfaces and absorption losses in ITO and CdS, front and rear surface recombination losses of CdTe as well as recombination losses in SCR have been studied. It has been observed that the short-circuit current strongly depends on the thickness of ITO, thickness of CdS, thickness CdTe and electron lifetime. The concentration of uncompensated impurities (Na−Nd) in CdTe, which determines the width of SCR, plays a key role in the generation of photocurrent. The recombination losses in the SCR decrease rapidly with increasing the carrier lifetime in this region and can be ignored at lifetime of 10^{-7} s. The reflectivity from the back contact introduces a small influence in increasing the short-current density particularly at thick absorber layer (5–8 ȝm). Under the conditions of $Na - Nd \sim 10^{16}$ cm^{-3}, $\tau_n = 10^{-6}$ s, d_{CdTe} = 8ȝm, d_{ITO} = 100 nm, and d_{CdS} = 100 nm, the recombination and optical losses record their minimum ratio of 27%. Most of these losses (24%) are due to the optical losses. The efficiency of CdS/CdTe under these parameters is about 18.2% which is exactly matching with the recent experimental studies. Moreover, an ultrathin CdTe (=1 ȝm) is sufficient to introduce high efficiency of 16.4%.

Thin Solid Films 589(2015)72-78

Optical study of the vibrational and dielectric properties of $BiMnO_3$

W. S. Mohamed[1], A. Nucara, G. Calestani, F. Mezzadri, E. Gilioli F. Capitani, P. Postorino, and P. Calvani.

[1]*Physics Department, Faculty of Science, Sohag University, 82524-Sohag, Egypt*

$BiMnO_3$ (BMO), ferromagnetic (FM) below Tc = 100 K, was believed to also be ferroelectric (FE) due to a noncentrosymmetric C2 structure, until diffraction data indicated that its space group is the centrosymmetric C2/c. Here we present infrared phonon spectra of BMO, taken on a mosaic of single crystals, which are consistent with C2/c at any T >10 K, as well as room-temperature Raman data which strongly support this conclusion. We also find that the infrared intensity of several phonons increases steadily for $T \rightarrow 0$, causing the relative permittivity of BMO to vary from 18.5 at 300 K to 45 at 10 K. At variance with FE materials of the displacive type, no appreciable softening has been found in the infrared phonons. Both their frequencies and intensities, moreover, appear insensitive to the FM transition at T_c.

PHYSICAL REVIEW B 92, 054306 (2015)

Raman phonon spectrum of the Dzyaloshinskii-Moriya helimagnet $Ba_2CuGe_2O_7$

F. Capitani, S. Koval, R. Fittipaldi, S. Caramazza,E. Paris, W. S. Mohamed[1], J. Lorenzana,A. Nucara, L. Rocco, A. Vecchione, P. Postorino, and P. Calvani.
[1]*Physics Department, Faculty of Science, Sohag University, 82524-Sohag, Egypt*

The Raman spectrum of $Ba_2CuGe_2O_7$, a tetragonal insulator which develops Dzyaloshinskii-Moriya helical magnetism below T_N = 3.2 K, has been detected at temperatures varying from 300 to 80 K in a single crystal, with the radiation polarized either in the *ab* plane or along the *c* axis of its tetragonal cell. Twenty-nine phonon lines out of the 35 allowed by the Raman selection rules for the present geometry were observed, and their vibrational frequencies were found in overall good agreement with those provided by shell-model calculations. Together with the previous report on the infrared-active phonons [A. Nucara *et al.*, Phys. Rev. B **90**, 014304 (2014)], the present study provides an exhaustive description, both experimental and theoretical, of the lattice dynamics in $Ba_2CuGe_2O_7$.

PHYSICAL REVIEW B 91, 214308 (2015)

Structural and electrical properties of $In_{35}Sb_{45}Se_{20-x}Te_x$ chalcogenide thin films

A.K. Diab, M.M. Wakkad, E.Kh. Shokr, W.S. Mohamed
Physics Department, Faculty of Science, Sohag University, 82524-Sohag, Egypt

The structural and electrical properties of the as-prepared and annealed $In_{45}Sb_{35}Se_{20-x}Te_x$ thin films with different compositions (x = 2.5, 5, 7.5, 10, 12.5 and 15 at.%) prepared by electron beam evaporation method are studied. The XRD patterns of the as-prepared thin film show that the investigated compositions have amorphous and polycrystalline structure depending on the Te content. After annealing the $In_{35}Sb_{45}Se_{20-x}Te_x$ thin films, at 473 K for 10 min, crystalline peaks are obtained. The electrical measurements were taken during heating in the range from 300 to 600 K. It was found that the resistivity decreases with increasing temperature for all the compositions indicating that these films have a semiconducting behavior. After annealing it was found that the room temperature resistivity of the investigated films were found depend on annealing temperature which cause a reduction by five orders of magnitude. These can be attributed to the amorphous–crystalline transformation, which is accompanied by a pronounced change in the electronic structure.

Optik 126, 19 (2015)

Kinetics of Ion Formation in Rubidium Vapour Excited by Nanosecond Resonant Laser Pulses

M.A.Mahmoud[1] and Y.E.E.Gamal[2]
[1]*Department of Physics, Faculty of Science, Sohag University, Sohag 82524, Egypt*
[2]*National Institute of Laser Enhanced Science, Cairo University, El Giza, Egypt*

We have studied theoretically formation of molecular ion Rb_2^+ and the atomic ion Rb^+ which are created in laser excited rubidium vapor at the $5S_{1/2} \rightarrow 5P_{3/2}$ or $5S_{1/2} \rightarrow 5P_{1/2}$,λ_{D1}=780 nm ,λ_{D2}=795 nm) . A set of rate equations ,which describe the temporal variation of the electron energy distribution function(EEDF), the electron density, the population density of the excited states as well as the atomic Rb^+ and molecular ion Rb^+_2 ,are solved numerically . The calculations are carried out at different laser energy and different rubidium atomic vapor densities. The numerical calculations show that competition between associative ionization(5p-5p),and Molnar –Hornbeck ionization processes for producing Rb_2^+.,the calculations have also shown that the atomic ions Rb^+ are formed through the Penning ionization and photoionization processes . Also, the obtained results showed reasonable agreement with the experimentally measured values of the ion density dependence given by Bakhramov et al(2002).

32nd ICPIG, July 26-31, 2015, Iași, Romania.

Ionization of lithium vapor by nanosecond resonant laser pulses tuned to 2S - 2P transition

M A Mahmoud[1], M A Khedr and M Nady,
[1]*Physics department, Faculty of Science, Sohag University,82524-Sohag,Egypt.*
[2]*National Institute of Laser Enhanced Science, Cairo University, El Giza, Egypt*

A theoretical study is reported for the resonant excitation and ionization of dense lithium vapor induced by nanosecond laser pulses tuned to the resonance transition *2S-2P* . The lithium vapor with density (10^{14} -10^{16} cm^{-3}) is assumed to be excited and ionized by a laser beam with laser power of (10^{5} -10^{6} Wcm^{-2}) according to the experimental conditions of Skenderovic et al[Phys.Rev A **62** 052707 (2000)]. The time evolution of electron energy distribution function and the electron density , the population density of the excited states as well as the atomic ion ,are solved numerically. The numerical calculations of the electron energy distribution function show that nonequilibrium plasmas are produced in lithium vapor by laser irradiation of the *nS – nP* resonance line .The electrons in these plasmas are heated by superelastic collisions with atoms in the *nP* state giving a distribution of electrons in energy that is characterized by a series of spikes at energy separated by the *nS – nP* transition energy. In addition, the competition between photoionization processes and collisional ionization processes for producing the Li^{+} as well as energy pooling collisions process of the excited lithium atoms play essential roles in populating the highly excited states .Moreover, the results are found to be consistent with the experimental observations.

Indian J Phys,89 (2015) 89(7)743.

Influence of intermediate ηNN interaction on spin asymmetries for γd → π^0d reaction near the η-threshold within a three-body approach

Eed M. Darwish[1,2], and A. Hemmdan[3]
[1]*Physics Department, Faculty of Science, Sohag University, Egypt*
[2]*Physics Department, Faculty of Science, Taibah University, Saudi Arabia*
[3]*Physics Department, Faculty of Science, Aswan University, Egypt*

The influence of intermediate ηNN interaction on spin asymmetries for coherent π^0-photoproduction on the deuteron in the energy region around the η-threshold is studied using a three-body model with separable two-body interactions. We calculate all possible spin asymmetries with polarized photons and/or oriented deuterons and compare our results with available data. The calculations are based on a theoretical approach which includes the amplitudes of the impulse approximation, two-body process with πN- and ηNrescattering, and the higher order terms in the multiple scattering series for the intermediate ηNN interaction. We found that the results for spin asymmetries of the differential cross section differ significantly from those calculated by a simple model in which only the impulse approximation and first-order rescattering contributions are considered. The effect of intermediate ηNN interaction is significant in certain spin asymmetries, specially at extreme backward pion angles. It turns out that the inclusion of a full ηNN three-body contribution is quite essential. The spin asymmetries of the total cross section are much less affected by rescattering contributions. Compared to the experimental data from YerPhi Collaboration for the linear photon asymmetry, sizeable discrepancies are found.

Annals of Physics, Vol. 356, 128-148 (2015)

Helicity-dependent reaction γ d → π ^{0}d near the η-threshold and its contribution to the E-asymmetry and the GDH sum rule for the deuteron

Eed M. Darwish[1,2], A. Hemmdan[3] and N.T. El-Shamy[2,4]
[1]Physics Department, Faculty of Science, Sohag University, Egypt
[2]Physics Department, Faculty of Science, Taibah University, Saudi Arabia [3]Physics Department, Faculty of Science, Aswan University, Egypt
[4]Physics Department, Faculty of Girls, Ain Shams University, Egypt

The helicity-dependent coherent π ^{0} -photoproduction in the reaction γd → π ^{0}d near the η-threshold is investigated. The calculations are performed within an approach which includes the reaction amplitudes of the impulse approximation, two-step process with intermediate πN- and ηN-rescattering, and the higher order terms in the multiple scattering series for the intermediate ηNN interaction. The contribution of γd → π ^{0}d to the deuteron spin asymmetry is calculated and its contribution to the GDH integral is explicitly evaluated by integration up to a photon energy of 900 MeV. In addition, the helicity E-asymmetry is calculated. The results revealed that the doubly polarized differential cross sections and the helicity E-asymmetry are sensitive to the interference of rescattering effects, specially at photon energies 600- 800 MeV and extreme backward pion angles. The sensitivity of the obtained results for the GDH integral to the choice of NN potential model governs the deuteron wave function is discussed. We find that the deviation among results obtained for the deuteron GDH integral using different deuteron wave functions is quite large.

International Journal of Modern Physics E, 24 (8), (2015) 1550064

Sensitivity of γd → π ^{0}d observables near η-threshold to the intermediate ηNN interaction and the choice of elementary pion production amplitude

Eed M. Darwish[1,2],∗ and S.S. Al-Thoyaib[3]
[1]Physics Department, Faculty of Science, Sohag University, Egypt
[2]Physics Department, Faculty of Science, Taibah University, Saudi Arabia [3]Physics Department, Faculty of Science, Qassim University, Saudi Arabia

The role of intermediate ηNN interaction is studied in coherent π^0 -photoproduction on the deuteron near η-threshold using a three-body model with separable two-body interactions. This work is motivated by the measurements of the CLAS Collaboration at Jefferson laboratory, where a cusp-like structure in the energy dependence of the differential cross section has been observed at extremely backward pion angles. Results for differential and total cross sections are predicted and compared with available data. We found that the results for differential cross section differ significantly from those predicted by a simple model in which only the impulse approximation and two-body process contributions are considered. In addition, the sensitivity of the results for unpolarized cross sections and polarization observables to the elementary amplitude is investigated and considerable dependences are obtained. The results revealed that the intermediate ηNN three-body calculation and the choice of the elementary amplitude have a visible effect on the differential cross section and spin asymmetries. Compared to the experimental data from CLAS Collaboration for differential cross section, sizeable discrepancies are found.

Journal of the Physical Society of Japan, 84 (2015) 124201

Review of polarization observables in incoherent pion photoproduction on the deuteron

Eed M. Darwish[1,2]
[1]*Physics Department, Faculty of Science, Sohag University, Egypt*
[2]*Physics Department, Faculty of Science, Taibah University, Saudi Arabia*

Polarization observables in incoherent pion photoproduction from the deuteron are investigated in the energy region from π-threshold up to the Δ(1232)- resonance with inclusion of all leading πNN effects. Formal expressions for polarization observables are derived and described by various beam, target and beam-target asymmetries for polarized photons and/or polarized deuterons. For the elementary pion photoproduction operator on the free nucleon, a realistic effective Lagrangian approach is used which includes seven nucleon resonances, in addition to Born and vector-meson exchange terms. The interactions in the final two-body subsystems are taken from separable representations of realistic potentials. Results are given for the unpolarized cross sections, the doubly polarized cross sections for parallel and antiparallel helicity states, the linear photon asymmetry, the double polarization E-asymmetry and, the vector and tensor deuteron asymmetries for the $\gamma\, d \rightarrow \pi^- pp$, $\gamma\, d \rightarrow \pi^+ nn$, and $\gamma d \rightarrow \pi^0 np$ channels. The contributions to the spin asymmetry and the Gerasimov-Drell-Hearn (GDH) integral from separate channels are evaluated by explicit integration up to a photon lab-energy of 350 MeV. Effects of final-state interaction are investigated and their role in these observables are found to be significant, specially for π^0 production. The extracted results are compared with available experimental data and predictions of other works, and a satisfactory agreement is obtained. The sensitivity of the $\gamma d \rightarrow \pi NN$ results to the elementary $\gamma N \rightarrow \pi N$ operator is also investigated and a considerable dependence is found. This indicates that it can serve as a filter for different elementary operators. We expect that the results presented here may be useful to interpret the recent measurements from the high-intensity and high duty-factor electron accelerators MAMI, ELSA, Jefferson Lab, LEGS, and MAX-Lab.

Applied Mathematics & Information Science, 9 (2), (2015) 527-548

Influence of double scattering effects on the γd → π^0d reaction near the η-threshold

Eed M. Darwish[1,2],∗ and A.S. Aldobuani[3]
[1]Physics Department, Faculty of Science, Sohag University, Egypt
[2]Physics Department, Faculty of Science, Taibah University, Saudi Arabia [3]Physics Department, Faculty of Science, King Abdulaziz University, Saudi Arabia

The influence of double scattering effects on coherent π 0 -photoproduction on the deuteron is studied in the energy region near the η-production threshold at backward center-of-mass angles of the outgoing pion. The model is based on the impulse approximation and double scattering diagrams with intermediate production of both π- and η-mesons. Numerical results for the differential cross section and tensor target asymmetries are predicted and compared with available experimental data and other theoretical models. The effects of double scattering are found to be much larger in the tensor target asymmetries than in the differential cross section. Compared to the experimental data from CLAS Collaboration, sizeable discrepancies are found.

Quantum Information Review, 3(1) (2015) 1-7

Contribution of coherent and incoherent π-photoproduction channels to the spin asymmetry and the GDH sum rule for the deuteron

Eed M. Darwish[1,2]
[1]*Physics Department, Faculty of Science, Sohag University, Egypt*
[2]*Physics Department, Faculty of Science, Taibah University, Saudi Arabia*

An explicit evaluation of the deuteron spin asymmetry and the associated GDH integral for coherent and incoherent π-photoproduction channels with inclusion of rescattering effects is presented. The helicity-dependent total inclusive photoabsorption cross section on the deuteron and the helicitydependent semi-exclusive channels $\gamma d \rightarrow \pi \pm NN$ and $\gamma d \rightarrow \pi^0 X$ (X = pn or d) are explicitly evaluated up to 1.5 GeV. Our model calculations indicate that convergence of the GDH integral is reached for π^0-production, but it is not completely reached for π ±-production. For the sum of $\gamma d \rightarrow \pi NN$ and $\gamma d \rightarrow \pi^0 d$ contributions to the finite GDH integral by explicit integration up to 1.5 GeV, a value of 249.73 μb is obtained. The extracted results are compared with available experimental data from MAMI and ELSA. We found that our predictions fairly well reproduce the data in the π ±NN case, but fail to predict the measured shape of the $\pi^0 X$ channel.

Chinese Physics Letters, 32 (12), (2015) 122501

Incoherent pion photoproduction on the deuteron: A review

Eed M. Darwish[1,2]
[1]*Physics Department, Faculty of Science, Sohag University, Egypt*
[2]*Physics Department, Faculty of Science, Taibah University, Saudi Arabia*

Polarization observables in incoherent pion photoproduction on the deuteron are investigated in the energy region from π-threshold up to the Δ(1232)- resonance with inclusion of all leading πNN effects. Formal expressions for polarization observables are derived and described by various beam, target and beam-target asymmetries for polarized photons and/or polarized deuterons. For the elementary pion photoproduction operator on the free nucleon, a realistic effective Lagrangian approach is used which includes seven nucleon resonances, in addition to Born and vector-meson exchange terms. The interactions in the final two-body subsystems are taken from separable representations of realistic potentials. Results are given for the unpolarized cross sections, the doubly polarized cross sections for parallel and antiparallel helicity states, the linear photon asymmetry, the double polarization E-asymmetry and, the vector and tensor deuteron asymmetries for the $\gamma d \to \pi^- pp$, $\gamma d \to \pi^+ nn$, and $\gamma d \to \pi^0 np$ channels. The contributions to the spin asymmetry and the Gerasimov-Drell-Hearn (GDH) integral from separate channels are evaluated by explicit integration up to a photon lab-energy of 350 MeV. Effects of final-state interaction are investigated and their role in these observables are found to be significant, specially for π^0 production. The extracted results are compared with available experimental data and predictions of other works, and a satisfactory agreement is obtained. The sensitivity of the $\gamma d \to \pi NN$ results to the elementary $\gamma N \to \pi N$ operator is also investigated and a considerable dependence is found. This indicates that it can serve as a filter for different elementary operators. We expect that the results presented here may be useful to interpret the recent measurements from the high-intensity and high duty-factor electron accelerators MAMI, ELSA, Jefferson Lab, LEGS, and MAX-Lab.

LAMBERT Academic Publishing, ISBN: 978-3-659-68847-8 (2015)

Coherent π-production off deuteron near η-threshold: A theoretical overview

Eed M. Darwish[1,2], and H.M. Mansour[3]
[1]Physics Department, Faculty of Science, Sohag University, Egypt
[2]Physics Department, Faculty of Science, Taibah University, Saudi Arabia [3]Physics Department, Faculty of Science, Cairo University, Egypt

Coherent π^0 -photoproduction off the deuteron near η-threshold is investigated within an approach which includes the reaction amplitudes of the impulse approximation, two-step process with intermediate πN- and ηNrescattering, and the higher order terms in the multiple scattering series for the intermediate ηNN interaction. Results for unpolarized and polarized cross sections as well as for all possible polarization observables with polarized photons and/or oriented deuterons are predicted and compared with available data, and differences with other theoretical models are analyzed. The contribution of $\gamma d \rightarrow \pi^0 d$ to the deuteron spin asymmetry is calculated and its contribution to the Gerasimov-Drell-Hearn (GDH) integral is explicitly evaluated by integration up to a photon lab-energy of 900 MeV. In addition, the helicity E-asymmetry is calculated. This work is motivated by the measurements of the CLAS Collaboration at Jefferson laboratory, where a cusp-like structure in the energy dependence of the differential cross section has been observed at extremely backward pion angles. The effect of intermediate ηNN three-body interaction is significant in certain spin asymmetries, specially at extreme backward pion angles. It turns out that the inclusion of a full ηNN three-body contribution is quite essential. In addition, the sensitivity of the results to the elementary $\gamma N \rightarrow \pi^0 N$ amplitude and the choice of the NN potential model governs the deuteron wave function is also investigated and considerable dependences are obtained. Compared to the experimental data from CLAS Collaboration for differential cross section and from YerPhi Collaboration for the linear photon asymmetry, sizeable discrepancies are found.

LAMBERT Academic Publishing, ISBN: 978-3-659-81398-6 (2015)

Equation of State and Symmetry Energy at High Densities for Zero and Finite Temperatures

Khalaf Gad[1] and Hesham Mansour[2]
[1]*Physics Department, Faculty of Science, Sohag University, Sohag, Egypt*
[2]*Physics Department, Faculty of Science, Cairo University, Giza, Egypt*

The equation of state of isospin asymmetric nuclear matter within the framework of the Brueckner theory is used to calculate the energy per particle for nuclear and neutron matter. Pressure and symmetry energy are also presented. Here we extended our work to include Skyrme-like zero-range density-dependent two-body forces, which could mimic three body forces. A three-body forces are shown to be necessary for reproducing the empirical saturation properties of symmetric nuclear matter. We also studied the effect of extending the calculation to finite temperatures.

Journal of the Physical Society of Japan 84, (2015)

Nuclear and neutron matters at low density

Kh. Gad
Physics Department, Faculty of Science, Sohag University, Sohag, Egypt

In this study, symmetric and asymmetric nuclear matter, as well as pure neutron matter in the low-density regime, where the density ranges $0.01\ fm^{-3} \leq \rho \leq 0.13\ fm^{-3}$, have been investigated. Two different realistic and accurate two-body forces are considered. These include Argonne V18 and the CD-Bonn, which give quite different equations of state. The binding energy per nucleon as a function of the density is calculated using the Brueckner-Hartree-Fock approximation. Both the conventional (gap) and continuous choice of single-particle energies are utilized. For the sake of comparison, the equation of state within the self-consistent Green's function approach is calculated using the CD-Bonn potential. The contribution of the hole-hole terms leads to a repulsive contribution to the energy per nucleon which increases with the nuclear density. Significantly, very good agreement between the experimental symmetry energy values and those calculated in the self-consistent Green's function and BHF approaches especially at low density, has been accomplished. Finally, the results are compared with those from various many-body approaches, such as variational and relativistic mean field approaches.

Eur. Phys. J. A (2015) 51: 98

Single-Particle Properties of the Mirror Nuclei ^{48}Ca and ^{48}Ni from Realistic Nucleon–Nucleon Force

Khalaf Gad
Physics Department, Faculty of Science, Sohag University, Sohag, Egypt

Single-particle for the doubly magic nuclei ^{48}Ca and ^{48}Ni are calculated within the framework of the Green's function using the CD-Bonn, Argonne V18 and N^{3}LO nucleon–nucleon interactions. Both the continuous and conventional choices of single particle energies are used. Additional binding energy is obtained from the using the continuous choice. We also compare the binding energies obtained in this study with those obtained by various authors employing different method and techniques. The results show good agreement between the Green function calculated values using conventional choice and the experimental values for ^{48}Ni and ^{48}Ca nuclei. Also we found that, the proton-rich nucleus ^{48}Ni is less tightly bound by approximately 1.0 MeV per nucleon than its mirror nucleus ^{48}Ca, and this result is in good agreement with theoretical mass table evaluations.

Journal of the Physical Society of Japan 84, (2015) 064201

Single-Particle Spectrum of Pure Neutron Matter

Khalaf Gad[1] and Hesham Mansour[2]
[1]*Physics Department, Faculty of Science, Sohag University, Sohag, Egypt*
[2]*Physics Department, Faculty of Science, Cairo University, Giza, Egypt*

We have calculated the self-consistent auxiliary potential effects on the binding energy of neutron matter using the Brueckner–Hartree–Fock approach by adopting the Argonne V18 and CD-Bonn potentials. The binding energy with the four different choices for the self-consistent auxiliary potential is discussed. Also, the binding energy of neutron matter has been computed within the framework of the self-consistent Green's function approach. We also compare the binding energies obtained in this study with those obtained by various microscopic approaches. It is found that the use of the continuous choice tends to give binding energies about 2–4 MeV larger than the gap choice at $k_F = 1.8$ fm^{-1}. In the case of symmetric nuclear matter this difference is larger.

Journal of the Physical Society of Japan 84, (2015) 034201

Effect of Indium Alloying with Lead on the Mechanical Properties and Corrosion Resistance of Lead-Indium Alloys in Sulfuric Acid Solution

Abdel-Rahman, E.; Ibrahim, E. M. M.[1]; Mohran, H. S.; Ismael, M.; Shilkamy, H. A.
[1]*Physics Department, Faculty of Science, Sohag University, Sohag, Egypt*

Effect of indium alloying in various concentrations with lead on both microhardness and crystallite structure of lead-indium alloy was investigated. The corrosion behavior of leadindium alloys in 4 M H_2SO_4 acid solution was investigated by Tafel plot and electrochemical impedance spectroscopy (EIS) methods. The results of both Tafel plot extrapolation and EIS measurements exhibited the same trend. Generally, the corrosion resistance of the alloy is more significant compared with that observed for pure lead. This study shows that the addition of 0.5 pct In to Pb decreases the corrosion. However, with a further increase of alloying In, the corrosion rate of alloy starts to increase up to 5 pct In compared with that of Pb-0.5 pct In alloy. Then the corrosion rate decreases gradually with the increase in the percentage of In up to 15 pct. The values of activation energy (Ea) supported this trend of the corrosion rate which is obtained for Pb and Pb-In alloys. X-ray diffraction data exhibited broadness of peaks, which is due to lattice distortion or grain refinement. Clearly the peaks shift to higher angles for Pb-15 pct In alloy which can be attributed to changes in lattice structure of Pb. Scanning electron microscope images confirmed that the microstructure is changed with indium alloying content. The solute content tends to refine the microstructure array.

Metallurgical and Materials Transactions A, 46 (2015) 1995 - 2006.

Tailor-made carbon nanostructures for practical applications

V. O. Khavrus, T. Sobolkina, S. Hampel, R. Ummethala, E.M.M. Ibrahim[1], A. Leonhardt,
[1]Physics Department, Faculty of Science, Sohag University, Sohag, Egypt

In this paper, we report conditions of the simultaneous, but separated, deposition of single- and multiwalled carbon nanotubes (SWCNTs, MWCNTs) in one and the same CVD process by a thermal decomposition of acetonitrile and ferrocene at different ratios. We have found an effective separation between SWCNTs and MWCNTs inside the reactor. The MWCNTs are formed on the hot reactor wall, whereas the SWCNTs are spontaneously originated in the gas phase. By means of an argon gas flow, they are transported through the quartz tube reactor and collected on a cooling finger. The morphology and purity of the pristine material are dependent on the amount of evaporated acetonitrile and C/Fe ratio in the gas phase. The reasons for the observed phenomena are discussed.

Conference: Our portfolio and new ideas, 24-25 February 2015, Würzburg, Germany

Effect of heat treatment on the electrical and thermoelectric properties of Sb doped Bi_2Se_3,

E M M Ibrahim, A M Abdel Hakeem, A M M Adam and E Kh Shokr
Physics Department, Faculty of Science, Sohag University, Sohag, Egypt

Polycrystalline samples of (Bi0.95Sb0.05)2Se3 were prepared using the conventional melting technique at 1273 K, followed by annealing at different temperatures (423, 473, 523 and 573 K) for different time intervals (4, 8, 12 and 16 h). The samples were crystallized in a single phase of Bi2Se3 and no other phases or impurities were observed. The electrical and thermoelectric properties were studied by measuring the electrical conductivity and Seebeck coefficient as functions of temperature in the range 100–400 K. The results exhibited a metal–n-type semiconductor transition for all samples. The power factor (Pf) was calculated to determine the effect of the annealing treatment on the performance of the prepared material as a thermoelectric power generator. The highest room temperature value of the Pf was 6.9 ₃WK−2cm^{-1} and was recorded for the sample annealed at 573 K for 16 h. The results confirm the feasibility of using the annealing process to improve the performance of thermoelectric materials.

Phys. Scr. 90 (2015) 045802

Study of multiplicity correlations in nucleus–nucleus interactions at high energy

M. Mohery[1,2] E. M. Sultan[2] and Shadiah S. Baz[3]

[1]Physics Department, Faculty of Science, North Jeddah, King Abdulaziz University, Jeddah, Saudi Arabia / [2]Physics Department, Faculty of Science, Sohag University, Sohag, Egypt / [3]Physics Department, Girls Faculty of Science, King Abdulaziz University, Saudi Arabia

In the present paper, some results on the correlations of the nucleus–nucleus interactions, at high energy, between different particle multiplicities are reported. The correlations between the multiplicities of the different charged particles emitted in the interactions of ^{22}Ne and ^{28}Si nuclei with emulsion at (4.1–4.5)A GeV/c have been studied. The correlations of the compound multiplicity nc, defined as the sum of both numbers of the shower particles ns and grey particles ng, have been investigated. The experimental data have been compared with the corresponding theoretical ones, calculated according to the modified cascade evaporation model (MCEM). An agreement has already been fairly obtained between the experimental values and the calculated ones. The dependence of the average compound multiplicity, on the numbers of shower, grey, black and heavy particles is obvious and the values of the slope have been found to be independent of the projectile nucleus. On the other hand, the variation of the average shower, grey, black and heavy particles is found to increase linearly with the compound particles. A strong correlation has been observed between the number of produced shower particles and the number of compound particles. Moreover, the value of the average compound multiplicity is found to increase with the increase of the projectile mass. Finally, an attempt has also been made to study the scaling of the compound multiplicity distribution showing that the compound multiplicity distribution is nearly consistent with the KNO scaling behavior.

International Journal of Modern Physics E Vol. 24, No. 6 (2015) 1550048

Effect of oxygen doping on the structure of TiN surface coatings

Domokos BIRÓ[1a], László JAKAB-FARKAS[1b], András KELEMEN[1b] , Sándor PAPP[1b] , Mohamed Fathy HASANEEN[2] , Miklós MENYHÁRD[2] , Sándor GURBÁN[2] , Péter B. BARNA[2]

[1a]Department of Mechanical Engineering, Faculty of Technical and Human Sciences, Sapientia University, Tg. Mureş,

[1b]Department of Electrical Engineering, Faculty of Technical and Human Sciences, Sapientia University, Tg. Mureş,

[2]Institute for Technical Physics and Materials Science, Centre for Energy Research, Hungarian Academy of Sciences, H-1525 Budapest, Po Box 49, Hungary

In the present work the influence of the level of oxygen doping on the structure of TiN films was investigated by dedicated experiments. The films were deposited at 400^{o}C in an all metal UHV device by unbalanced magnetron sputtering at the same Ar and nitrogen flow rates, but the oxygen flow rate was changed in the experiments, incorporating oxygen in the range of 4 and 20 at.%. The structure of the films was investigated by XRD, Auger electron (AES) and X-ray photon electron (XPS) spectroscopy and transmission electron microscopy (TEM). The results discovered the crystal face anisotropy in the incorporation-segregation of oxygen leading to the change of the texture to. The structure analysis revealed that the texture is developing also by competitive growth of crystals, which is the result of the limitation of the growth of the oriented crystals by the TiO_2 layer developing on their growth surface by the segregated oxygen species. The oxygen incorporating in the crystal lattice on the 002 crystal faces of the oriented crystals is segregated by surface spinodal decomposition, developing nm sized 3D TiO_2 inclusion both in the bulk of the columns and the column boundaries.

MACRo 2015- 5th International Conference on Recent Achievements in Mechatronics, Automation, Computer Science and Robotics

Study of multiplicity correlations in nucleusnucleus interactions at high energy

M (Mohery, M.) [1,2] ; Sultan, EM (Sultan, E. M.) [2] ; Baz, SS (Baz, Shadiah S.) [3]
[1] *King Abdulaziz Univ, Fac Sci, Dept Phys, Jeddah 21413, Saudi Arabia*
[2] *Sohag Univ, Fac Sci, Dept Phys, Sohag, Egypt*
[3] *King Abdulaziz Univ, Girls Fac Sci, Dept Phys, Jeddah 21413, Saudi Arabia*

In the present paper, some results on the correlations of the nucleusnucleus interactions, at high energy, between different particle multiplicities are reported. The correlations between the multiplicities of the different charged particles emitted in the interactions of Ne^{22} and Si^{28} nuclei with emulsion at (4.14.5) A GeV/c have been studied. The correlations of the compound multiplicity n(c), defined as the sum of both numbers of the shower particles n(s) and grey particles n(g), have been investigated. The experimental data have been compared with the corresponding theoretical ones, calculated according to the modified cascade evaporation model (MCEM). An agreement has already been fairly obtained between the experimental values and the calculated ones. The dependence of the average compound multiplicity, on the numbers of shower, grey, black and heavy particles is obvious and the values of the slope have been found to be independent of the projectile nucleus. On the other hand, the variation of the average shower, grey, black and heavy particles is found to increase linearly with the compound particles. A strong correlation has been observed between the number of produced shower particles and the number of compound particles. Moreover, the value of the average compound multiplicity is found to increase with the increase of the projectile mass. Finally, an attempt has also been made to study the scaling of the compound multiplicity distribution showing that the compound multiplicity distribution is nearly consistent with the KNO scaling behavior.

International Journal of Modern Physics Nuclear Physics, 24 (6) 2015

Chemistry

Effect of nickel content on the anodic dissolution and passivation of zinc–nickel alloys in alkaline solutions by potentiodynamic and potentiostatic techniques

Abdel-Rahman El-Sayed, Hany M Abd El-lateef* and Hossnia S Mohran
Chemistry Department, Faculty of Science, Sohag University, Sohag 82524, Egypt

The effect of systematic increase of Ni on the anodic dissolution and passivation of Zn–Ni alloys in various concentrations of KOH solution (0.1–1 M) was investigated. The anodic dissolution and passivation behaviour for each pure Zn and Ni in the same studied solutions was also investigated, and the obtained data were compared. Potentiodynamic and potentiostatic methods were used, and the corrosion layer formed on each electrode surface was characterized by X-ray diffraction (XRD) and scanning electron microscope (SEM). The results of the anodic potentiodynamic measurements exhibited that the polarization curves showed active/passive transition in the case of Ni and active/pseudopassive in the case of both Zn and its alloys. The results showed that the increase in Ni content increases the activation energy (E a) and decreases the dissolution rate of the alloys in KOH solution, and the low- est dissolution rate was obtained at 10% Ni. The results of both potentiodynamic and potentiostatic measurements exhibit sudden increase in current density which is observed at certain positive potential (+0.42 V vs. SCE) in the case of the investigated alloys. This indicates that the addition of Ni to Zn promotes the electrochemical reaction (in the passive region). However, the passivation potential shifted to more positive direction with the increase in Ni content in the alloy.

Bull. Mater. Sci., 38 (2015) 1–13, DOI: 10.1007/s12034-014-0814-7

Novel Schiff base amino acid as corrosion inhibitors for carbon steel in CO_2 -saturated 3.5% NaCl solution: experimental and computational study

Hany M. Abd El-Lateef*, Mohamed Ismael and Ibrahim M.A. Mohamed
Chemistry Department, Faculty of Science, Sohag University, Sohag 82524, Egypt

The corrosion inhibition and adsorption behaviour of some novel Schiff bases based on amino acids on car- bon steel in CO_2-saturated 3.5% NaCl solution at 50 °C was investigated using gravimetric, potentiodynamic polarization, linear polarization resistance corrosion rate, and scanning electron microscope (SEM)/energy-dispersive X-ray spectroscopy analysis (EDAX) techniques. Results show that the inhibition efficiency increases when the inhibitor concentration increases. Potentiodynamic polarization curves reveal that the used Schiff bases are mixed- type inhibitors. Experimental data indicate that these Schiff base inhibitors adsorb at the carbon steel/solution interface according the Langmuir adsorption isotherm. SEM/EDAX was used to examine the surface morphology of carbon steel samples in the absence and presence of the inhibitors. Quantum chemical calculations were further applied to explain the experimental results.

Corros Rev, 33(1-2) (2015) 77–97, DOI: 10.1515/corrrev-2014-0059

Experimental and computational investigation on the corrosion inhibition characteristics of mild steel by some novel synthesized imines in hydrochloric acid solutions

Hany M. Abd El-Lateef
Chemistry Department, Faculty of Science, Sohag University, Sohag 82524, Egypt

Two novel imines were synthesized and their inhibitive properties on mild steel corrosion in HCl were investigated using potentiodynamic polarization, electrochemical impedance spectroscopy and linear polarization resistance corrosion rate. Polarization curves indicate that all studied compounds were acting as mixed type inhibitors. All measurements showed that, inhibition efficiencies increase with increasing inhibitor concentration. Adsorption of these inhibitors follows Langmuir adsorption isotherm. The potential of zero charge in inhibited solution was studied, and a mechanism for the adsorption process was proposed. Theoretical calculations have been used to provide the correlation between the inhibition efficiencies of studied inhibitors and their molecular structure.

Corrosion Science 92 (2015) 104–117, DOI: 10.1016/j.corsci.2014.11.040

Investigation of adsorption and inhibition effects of some novel anil compounds towards mild steel in H_2SO_4 solution: Electrochemical and theoretical quantum studies

Hany M. Abd El-Lateef [a],*, Ahmed M. Abu-Dief [a], Bahaa El-Dien M. El-Gendy[b]
[a]*Chemistry Department, Faculty of Science, Sohag University, 82524 Sohag, Egypt*
[b]*Chemistry Department, Faculty of Science, Benha University, 13518 Benha, Egypt*

A novel anil compounds, 1-{(*Z*)-[(3,5dimethylphenyl)imino]methyl}naphthalen-2-ol **(HNMA)** and 5- (diethylamino) -2- {(*Z*)- [(3,5-dimethylphenyl)imino] methyl} phenol **(DMSMA)**, were prepared and characterized on the basis of elemental analyses, X-ray, ^{1}H NMR, ^{13}C NMR, UV-Vis and IR spectral data. Their inhibiting performance for mild steel in 0.5 M H_2SO_4 solution was evaluated by a series of techniques including potentiodynamic polarization, electrochemical impedance spectroscopy, scanning electronic microscope (SEM), energy-dispersive X-ray spectroscopy (EDX) and theoretical calculations. Findings show that **HNMA** and **DMSMA** act as good inhibitors, and their inhibition efficiency increases with increasing their concentration. Polarization data suggested that the Schiff bases molecules used as mixed type inhibitors. Impedance measurements indicating that the corrosion reaction is controlled by charge transfer process. The **HNMA** and **DMSMA** adsorption on metal surface obeys Langmuir adsorption isotherm. Furthermore, theoretical study gives insightful explanations of the inhibition mechanism.

Journal of Electroanalytical Chemistry 758 (2015) 135–147, DOI: doi.org/10.1016/j.jelechem.2015.10.025

Novel naphthenate surfactants based on petroleum acids and nitrogenous bases as corrosion inhibitors for C1018-type mild steel in CO_2-saturated brine

Hany M. Abd El-Lateef [a]*, V. M. Abbasov[b] , L. I. Aliyeva[b] , Mai M. Khalaf[a]
[a]*Chemistry Department, Faculty of Science, Sohag University, 82524 Sohag, Egypt*
[b]*Mamedaliev Institute of Petrochemical Processes, National Academy of Sciences of Azerbaijan, AZ1025 Baku, Azerbaijan*

The efficiency of two natural naphthenate surfactants (Naphthenic-dimethylamine and Naphthenic-diethylamine complexes), as corrosion inhibitors for mild steel in CO_2 -saturated 1% NaCl solution, has been determined by linear polarization resistance corrosion rate and potentio- dynamic polarization measurements. These compounds inhibit corrosion even at very low concentrations (25 ppm), and Naphthenic-diethylamine complex is the best inhibitor giving maximum inhibition efficiency (99.76) at 100 ppm. Polarization curves indicate that, the two investigated com- pounds are mixed inhibitors, affecting both cathodic and anodic corrosion currents. Adsorption of naphthenate surfactants on the mild steel surface is in good agreement with the Langmuir adsorption isotherm model, and the calculated Gibbs free energy values confirm the chemical nature of the adsorption. Energy dispersive X-ray fluorescence microscopy (EDRF) and scanning electron micro- scope (SEM) observations confirmed the existence of such an adsorbed film on the mild steel surface.

Egyptian Journal of Petroleum 24 (2015) 175–182, DOI: org/10.1016/j.ejpe.2015.05.010

Effect of indium alloying with lead together with the addition of phosphoric acid in electrolyte to improve lead-acid battery performance

Abdel-Rahman El-Sayed*, Hossnia S. Mohran, Hany M. Abd El-Lateef, Hoda Abdel Shafy Shilkamy

Chemistry Department, Faculty of Science, Sohag University, 82524 Sohag, Egypt

The electrochemical and corrosion behavior of Pb and Pb-In alloys in both phosphoric and sulfuric acid solutions containing various concentrations of phosphoric acid (0.05 to 0.20 M) at different temperatures was studied. Tafel plot and electrochemical impedance spectroscopy (EIS) techniques were used to obtain the experimental data, and the corrosion products formed on the surface were characterized by scanning electron microscopy (SEM). The results of both Tafel plot extrapolation and impedance measurements showed the same trend. Minor indium (0.5%) alloying with lead significantly reduced corrosion rate in pure phosphoric acid solution. However, opposite behavior arises in the case of alloys containing indium more than 0.5%, that is, the corrosion is higher than that of lead and alloy I. The corrosion current density decreases in both Pb and alloy I (0.5%) in 4 M sulfuric acid with increasing the concentration of phosphoric acid up to 0.1 M, then starts to increase relatively with increasing the additive concentration up to 0.2 M (but still lower than that in pure H_2SO_4). This exhibits that the higher concentration (0.2 M) of H_3PO_4 is less inhibitive of alloy I corrosion in H_2SO_4 solution. However, addition of phosphoric acid in various concentrations to sulfuric acid having little influence to inhibit the corrosion of alloys containing higher indium content (1 to 15%). SEM photographs showed that, the presence of indium as a minor alloying element retards the formation of $PbSO_4$, but the formation of ù-PbO_2 enhances.

J Solid State Electrochem 19 (2015) 1463–1478, DOI: 10.1007/s10008-015-2765-3

Electrochemical and theoretical quantum approaches on the inhibition of C1018 carbon steel corrosion in acidic medium containing chloride using some newly synthesized phenolic Schiff bases compounds

Hany M. Abd El-Lateef [a]*, Ahmed M. Abu-Dief[a], L. H. Abdel-Rahman[a], Eva Carolina Sañudo[b], Núria Aliaga-Alcalde[c]

[a]*Chemistry Department, Faculty of Science, Sohag University, 82524 Sohag, Egypt*
[b]*Departament de Química Inorgànica, Universitat de Barcelona, Diagonal 645, 08028 Barcelona, Spain*
[c]*ICREA-Institut de Ciència de Materials de Barcelona (ICMAB-CSIC), Campus de la UAB, 08193 Bellaterra, Spain*

Two novel Schiff bases, 5-bromo-2-[(*E*)-(pyridin-3-ylimino)methyl]phenol (HBSAP) and 5-bromo-2-[(E)-(quinolin-8-ylimino)methyl]phenol **(**HBSAQ**)** have been synthesized. They have been characterized by elemental analysis and spectroscopic techniques (UV–Vis, IR and NMR). Moreover, the molecular structure of HBSAP and HBSAQ compounds are determined by single crystal X-ray diffraction technique. The inhibition activity of HBSAP and HBSAQ for carbon steel in 3.5 %NaCl+0.1 M HCl for both short and long immersion time, at different temperatures (20-50 ºC), was investigated using electrochemistry and surface characterization. The potentiodynamic polarization shows that, the inhibitors molecule is more adsorbed on the cathodic sites. Its efficiency increases with increasing inhibitor concentrations (92.8 % at the optimal concentration of 10^{-3} M for HBSAQ). Adsorption of the inhibitors on the carbon steel surface was found to obey Langmuir's adsorption isotherm with physical/chemical nature of the adsorption, as it is shown also by scanning electron microscopy. Further, the electronic structural calculations using quantum chemical methods were found to be in a good agreement with the results of the experimental studies.

Journal of Electroanalytical Chemistry 743 (2015) 120–133, DOI: org/10.1016/j.jelechem.2015.02.023

Corrosion resistance of ZrO_2–TiO_2 nanocomposite multilayer thin films coated on carbon steel in hydrochloric acid solution

Hany M. Abd El-Lateef, Mai M. Khalaf*

Chemistry Department, Faculty of Science, Sohag University, 82524 Sohag, Egypt

This work reports the achievement of preparing of x% zirconia (ZrO_2)–titania (TiO_2) composite coatings with different ZrO_2 percent on the carbon steel by dipping substrates in sol–gel solutions. The prepared coated samples were investigated by various surface techniques including X-ray diffraction (XRD), scanning electron microscopy (SEM), transmission electron microscopy (TEM) and energy dispersive X-ray spectroscopy (EDAX). Open-circuit potential (OCP), potentiodynamic polarization, and electrochemical impedance spectroscopy (EIS) methods were employed to investigate the corrosion resistance of the coated carbon steel substrates in 1.0M HCl solution at 50 °C. The data showed that, the corrosion protection property is not always proportional to the percent of ZrO_2. It can be inferred that there is an optimum percent (10%ZrO_2) for beneficial effects of loading ZrO_2 on the protection efficiency (98.70%), while higher loading percent of ZrO_2 in the sol–gel coating leads to the formation of a fragile film with poor barrier properties. EDAX/SEM suggests that the metal surface was protected through coating with ZrO_2–TiO_2 composite films.

Materials Characterization 108 (2015) 29–41, DOI: org/10.1016/j.matchar.2015.08.010

Role of Ni content in improvement of corrosion resistance of Zn−Ni alloy in 3.5% NaCl solution. Part I: Polarization and impedance studies

Hany M. Abd El-lateef*, Abdel-Rahman El-Sayed, Hossnia S. Mohran
Chemistry Department, Faculty of Science, Sohag University, 82524 Sohag, Egypt

Zinc plays an important role in the protection of iron and steel from corrosion in sea water; therefore, Ni alloying with Zn may be improved its corrosion resistance. Corrosion behavior of zinc-nickel alloys in synthetic sea water (3.5 wt. % NaCl) was studied using Tafel-plot and electrochemical impedance spectroscopy (EIS) techniques. The corrosion resistance of the investigated alloys with various contents (0.5 to 10 wt. % Ni) was compared with that of zinc. The results show that the corrosion resistance of zinc-nickel alloys (except 0.5 wt.% Ni) is superior to that of zinc. The 10 wt. % Ni gives the highest corrosion resistance due to the formation of Û–Zn_3Ni with Û–ZnNi phases in the alloy. In the case of alloy **I** (0.5 wt. % Ni), it exhibits a higher corrosion rate (less corrosion resistance) than that of Zn.

Trans. Nonferrous Met. Soc. China 25(2015) 2807-2816, DOI: 10.1016/S1003-6326(15)63906-1

Role of nickel alloying with Zinc on the anodic dissolution behavior of Zinc in 3.5% NaCl solution; Part II: Potentiodynamic, potentiostatic and galvanostatic studies

Hany M. Abd El-lateef*, Abdel-Rahman El-Sayed, Hossnia S. Mohran
Chemistry Department, Faculty of Science, Sohag University, 82524 Sohag, Egypt

Zinc is common metal used for steel protection from corrosion. The addition of further element, such as Ni, can modify the corrosion rate and maintain sacrificial protection. The study of the anodic dissolution behavior of Zn, Ni and Zn-Ni- alloys with different Ni content (from 0.5 to 10%) in 3.5% NaCl solution is investigated using potentiodynamic, potentiostatic and galvanostatic techniques. The composition and microstructure of the corrosion layer on Zn, Ni and Zn-Ni- alloys are characterized by energy-dispersive X-ray spectroscopy analysis (EDX) and scanning electron microscopy (SEM). The galvanostatic curves showed that the anodic behavior of all investigated electrodes exhibits active/passive transition and the tendency of the alloys to passivity decreases with increase in Ni content, except for $Zn_{99.5}$-$Ni_{0.5}$ alloy. While the potentiodynamic curves exhibited active passive transition only for pure Zn. Surface analysis revealed the presence of oxides, chlorides and metal hydroxide chloride in corrosion products, and very small cracks are observed for alloy IV compared with that of Zn.

Trans. Nonferrous Met. Soc. China 25(2015) 3152−3164, DOI: 10.1016/S1003-6326(15)63946-2

Enhanced corrosion inhibition of mild steel in CO_2 -saturated solutions containing some novel green surfactants based on cottonseed oil

I. T. Ismayilov, [1,2] Hany M. Abd El-Lateef, [2] V. M. Abbasov, [1] E. N. Efremenko, [3] L. I. Aliyeva [1] and Ch. K. Salmanova [1]

[1]*Mamedaliev Institute of Petrochemical Processes, National Academy of Sciences of Azerbaijan, AZ1025 Baku, Azerbaijan*

[2]*Chemistry Department, Faculty of Science, Sohag University, 82524 Sohag, Egypt*

[3]*Faculty of Chemistry, Lomonosov Moscow State University, 119991, GSP-1, 1-3 Leninskiye Gory, Moscow, Russia*

Some novel green surfactants based on cottonseed oil were synthesized and tested as inhibitors for the corrosion of mild steel in CO_2-saturated 1% NaCl solution by potentiodynamic polarization and linear polarization resistance corrosion rate measurements at 50°C. Their critical micelle concentrations at equilibrium in water at 25 °C were also determined. Inhibition efficiency increased with increase in the concentration of the studied surfactants, reached the maximum (99.34%) at 100 ppm. The Tafel polarization results indicate that the inhibitors act as mixed inhibitors. The adsorption of the inhibitors on the steel surface obeys Langmuir isotherms. The thermodynamic parameters of adsorption revealed a strong interaction between the inhibitors and the corroding mild steel surface.

Int. J. Corros. Scale Inhib., 4 (2015) 57-74, DOI: 10.17675/2305-6894-2015-4-1-057-074

Effect of Indium Alloying with Lead on the Mechanical Properties and Corrosion Resistance of Lead-Indium Alloys in Sulfuric Acid Solution

Abdel-Rahman El Sayed [1], Eslam M. M. Ibrahim[2], Hossnia S. Mohran[1], Mohamed Ismael[1], Hoda Abdel-Shafy Shilkamy[1]

[1]Chemistry Department, Faculty of Science, Sohag University, 82524 Sohag, Egypt
[2]Department of Physics, Faculty of Science, Sohag University, Sohag 82524, Egypt.

Effect of indium alloying in various concentrations with lead on both microhardness and crystallite structure of lead-indium alloy was investigated. The corrosion behavior of lead-indium alloys in 4 M H_2SO_4 acid solution was investigated by Tafel plot and electrochemical impedance spectroscopy (EIS) methods. The results of both Tafel plot extrapolation and EIS measurements exhibited the same trend. Generally, the corrosion resistance of the alloy is more significant compared with that observed for pure lead. This study shows that the addition of 0.5 pct In to Pb decreases the corrosion. However, with a further increase of alloying In, the corrosion rate of alloy starts to increase up to 5 pct In compared with that of Pb-0.5 pct In alloy. Then the corrosion rate decreases gradually with the increase in the percentage of In up to 15 pct. The values of activation energy (E_a) supported this trend of the corrosion rate which is obtained for Pb and Pb-In alloys. X-ray diffraction data exhibited broadness of peaks, which is due to lattice distortion or grain refinement. Clearly the peaks shift to higher angles for Pb-15 pct In alloy which can be attributed to changes in lattice structure of Pb. Scanning electron microscope images confirmed that the microstructure is changed with indium alloying content. The solute content tends to refine the microstructure array.

Metallurgical And Materials Transactions A, 46a (2015) 1995-2006, DOI: 10.1007/s11661-015-2827-2

Tailoring, physicochemical characterization, antibacterial and DNA binding mode studies of Cu(II) Schiff bases amino acid bioactive agents incorporating 5-bromo-2-hydroxybenzaldehyde

Ahmed M. Abu-Dief and Lobna A. E. Nassr

Chemistry Department, Faculty of Science, Sohag University, 82534 Sohag, Egypt
e-mail: ahmed_benzoic@yahoo.com

Five novel Cu(II) complexes derived from the condensation between 5 -bromosalicylaldehyde (bs) and α-amino acids (L-alanine, l-phenylalanine, L-aspartic acid, L-histidine and L-arginine) were synthesized and characterized by their elemental analyses, thermogravimetric analysis, IR, mass and electronic spectra, conductance and magnetic measurements. Moreover, the stoichiometry and the stability constants of the prepared complexes have been determined spectrophotometrically using continuous variation and molar ratio methods. The obtained results indicated that the Schiff bases of the amino acids: L-alanine, L-phenylalanine, L-histidine and L-arginine behave as tridentate ligands. The ligands are coordinating with the Cu(II) via azomethine nitrogen, deprotonated carboxylate oxygen and phenolic oxygen. However, in the case of L-aspartic, the ligand acts as tetradentate due to the coordination of the second carboxylate group. Based on the studies of magnetic moments and electronic spectra, a square planar geometry has been proposed for all Cu(II) complexes except bromsalicylaldehydine aspartate complex which has a distorted tetrahedral structure. The representative Schiff bases and their Cu(II) complexes were tested in vitro for their antibacterial activity against two Gram-positive bacteria (*Micrococcus luteus* and *Bacillus cereus)* and one Gram-negative bacteria (*Pseudomonas aeruginosa)*. All the complexes showed activity against the organisms more than the free Schiff base ligands and the activity increases with the increase in concentration of test solution containing the new complexes. Moreover, the interaction of the prepared Schiff base amino acid Cu(II) complexes with calf thymus DNA has been investigated by absorption spectra, viscosity and gel electrophoresis measurement and the mode of CT-DNA binding to the complexes has been explored. The investigated complexes exhibit cooperative binding and presumably intercalate into DNA and follow the trend: bsarc > bshc > bsalc > bsphalc > bsasc.

J IRAN CHEM SOC (2015) 12:943–955, DOI 10.1007/s13738-014-0557-9

Kinetic Screening for the Acid-Catalyzed Hydrolysis of Some Hydrophobic Fe(II) Schiff Base Amino Acid Chelates and Reactivity Trends in the Presence of Alkali Halide and Surfactant

Lobna A. E. Nassr and Ahmed M. Abu-Dief

Chemistry Department, Faculty of Science, Sohag University, 82534 Sohag, Egypt
e-mail: lobna.nassr@hotmail.com

Kinetics of acid-catalyzed hydrolysis of some high-spin Fe(II) Schiff base amino acid complexes were followed spectrophotometrically at 298 K under pseudo–first-order conditions. The studied ligands were derived from the condensation of 5 - romosalicylaldehyde with different four amino acids (phenylalanine, aspartic acid, histidine, and arginine). The acid hydrolysis reaction was studied in aqueous media and in the presence of different concentrations of the alkali halide (KBr) and cationic surfactant (cetyl-trimethyl ammonium bromide, CTAB). The general rate equation was suggested to be rate = *k*obs[complex], where *k*obs = $k_2[H^+]$. The increase in [KBr] enhances the reactivity of the reaction, and the addition of CTAB to the reaction mixture accelerates the reaction reactivity. The obtained kinetic data were used to determine the values of $\delta_m \Delta G^{\#}$ (the change in the activation barrier) for the studied complexes when transferred from ―water to water containing different [KBr] and from "water to water containing altered [CTAB]".

International Journal of Chemical Kinetics (2015) 1-8, DOI: 10.1002/kin.20927

Recent Advances in Synthesis, Characterization and Biological Activity of Nano Sized Schiff Base Amino Acid M(II) Complexes

Laila H. Abdel Rahman[a], Ahmed M. Abu-Dief[a], Nahla Ali Hashem[a] and Amin Abdou Seleem[b]

[a]Chemistry Department, Faculty of Science, Sohag University, 82534, Egypt

[b]Zoology Department, Faculty of Science, Sohag University, 82534 Sohag, Egypt

laila_kenawy@hotmail.com, ahmed_benzoic@yahoo.com

Azomethine amino ligands derived from the condensation of 3 -methoxysalicylaldehyde (MS) or 4-diethylaminosalicylaldehyde (DS) with α-amino acids (L-phenylalanine (P) and DL-tryptophan (T)) were synthesized. All ligands were analyzed by IR, ^{1}H NMR, ^{13}C NMR and their melting points. Interaction of the obtained azomethine amino ligands with metal salts produced novel nano sized Fe(II) and Cu(II) complexes. The isolated complexes were characterized by elemental analysis, infrared spectra, ultraviolet-visible and thermal analysis (TGA) in dynamic air atmosphere. The Kinetic and thermal parameters were computed from the thermal data using Coast and Redfern method. The molar conductance values of complexes are relatively low, indicating the non-electrolytic nature of the complexes. Magnetic susceptibility measurements show that the investigated complexes are paramagnetic. Moreover, the stability constants of the prepared complexes were determined spectrophotometrically. The analytical results suggest that amino acid Schiff bases behave as dibasic tridentate ONO ligands, and coordinate with Fe(II) and Cu(II) ions in octahedral geometry according to the general formula $[M(HL)_2].nH_2O$. The particle size of the prepared complexes was determined using TEM and it was found to be in nano scale. Moreover, the antimicrobial effects of the ligands and their complexes were screened against some types of bacteria such as *Bacillus subtilis (+ve)*, *Escherichia coli (-ve)* and *Micrococcusluteus (+ve)* and other types of fungi such as *Asperagillus niger*, *Candida glabrata* and *Saccharomyces cerevisiae*. The results of these studies indicate that the metal complexes exhibit a stronger antibacterial and antifungal efficiency compared to their corresponding ligands. The interaction of the complexes with CT-DNA was monitored using spectral studies, viscosity measurements and gel electrophoreses. Furthermore, it was found that the prepared complexes could bind to DNA in an intercalating mode.

Int. J. Nano. Chem. 1, No. 2, 79-95 (2015), http://dx.doi.org/10.12785/ijnc/010205

Salts and Structural Effects on the base Catalyzed Hydrolysis of some Novel and Pharmacologically Active Iron (II) Azomethine Amino Acid Complexes

Laila H. Abdel Rahman, Rafat EL-Khatib, Lobna A.E. Nassr, Ahmed M. Abu-Dief
Chemistry Department, Faculty of Science, Sohag University, Sohag, Egypt
E-mail: ahmed_benzoic@yahoo.com

The effect of salts on the reactivity of base hydrolysis of Fe(II) chelates bis(naphthylidene alanate) (nali), bis(naphthylidene phenylalanate) (nphali), bis(naphthylidene aspartate) (nasi), (naphthylidene histidinate) (nhi), bis(naphthylidene arginate) (nari) has been investigated in aqueous media containing alkali metal halides viz. LiBr, NaCl, KBr, Tetramethylammonium bromide (TMAB), Tetraethylammonium bromide (TEAB) and Tetrabutylammonium bromide (TBAB). The suggested mechanism of the base hydrolysis reaction involves the parallel attack of OH- ion on Fe2+ central atom attached to a singly bonded OH- ligand and dissociation of the first ligand as rate determining step. Generally, the presence of the salt markedly enhances the rate compared to its absence. This behavior agrees with the anionic nature of the transient species. With increasing added NaCl and NaBr, the rate of the reaction decreases. But in case of TMAB, TEAB and TBAB salts, the rate increases and then decreases on increasing their concentration.

Int. J. Nano. Chem. 1, No. 1, 25-30 (2015), http://dx.doi.org/10.12785/ijnc/010105

A review on versatile applications of transition metal complexes incorporating Schiff bases

Ahmed M. Abu-Dief[a,b]* and Ibrahim M. A. Mohamed[a]
[a]*Chemistry Department, Faculty of Science, Sohag University, Sohag, Egypt*
[b]*Departamento de Quimica Organica e Inorganica, Faculad de Quimica, Universdad de Oviedo, 33006 ,Oviedo ,Spain*
E-mail: ahmed_benzoic@yahoo.com

Schiff bases and their complexes are versatile compounds synthesized from the condensation of an amino compound with carbonyl compounds and widely used for industrial purposes and also exhibit a broad range of biological activities including antifungal, antibacterial, antimalarial, antiproliferative, anti-inflammatory, antiviral, and antipyretic properties. Many Schiff base complexes show excellent catalytic activity in various reactions and in the presence of moisture. Over the past few years, there have been many reports on their applications in homogeneous and heterogeneous catalysis. The high thermal and moisture stabilities of many Schiff base complexes were useful attributes for their application as catalysts in reactions involving at high temperatures. The activity is usually increased by complexation therefore to understand the properties of both ligands and metal can lead to the synthesis of highly active compounds. The influence of certain metals on the biological activity of these compounds and their intrinsic chemical interest as multidentate ligands has prompted a considerable increase in the study of their coordination behavior. Development of a new chemotherapeutic Schiff bases and their metal complexes is now attracting the attention of medicinal chemists. This review compiles examples of the most promising applied Schiff bases and their complexes in different areas.

Beni-Suef University Journal of Basic and Applied Sciences, 4 , 2015, 119-133, Doi.org/10.1016/j.bjbas.2015.05.004

Hydrophobicity and kinetic inspection of hydroxide ion attack on some chromen-2-one laser dyes in binary aqueous–methanol and aqueous–acetone mixtures: Initial state-transition state analysis

Ezz A. Abu-Gharib, Rafat EL-Khatib, Lobna A.E. Nassr, Ahmed M. Abu-Dief
Chemistry Department, Faculty of Science, Sohag University, Sohag, Egypt
E-mail: ahmed_benzoic@yahoo.com

2H-chromen-2-one (DMAC) and 7-diethylamino-4-methyl-2H-chromen-2-one (DEAC) in binary aqueous–methanol and aqueous–acetone mixtures was examined at 298 K. Kinetic results, rate laws and reaction mechanisms were established. Moreover, the change in the activation energy barrier of the investigated compounds from water to water–methanol and water–acetone mixtures was estimated from the kinetic data. Base-catalyzed hydrolysis of (DMAC) and (DEAC) in aqueous–methanol and aqueous–acetone mixtures follows a rate law with kobs= k_2[OH]. The decrease in the rate constants of (DMAC) and (DEAC) as the proportion of methanol and acetone is due to the destabilization of OH_ ion. The solubilities of the studied compounds, DMAC and DEAC in water–methanol and water–acetone mixtures were established and their transfer chemical potentials were calculated. Solvent effect on reactivity trends of the investigated compounds has been analyzed into initial and transition state components by using the transfer chemical potentials of the reactants and the kinetic data of the studied compounds. The decrease in the observed rate constant values (k_{obs}) of the base hydrolysis of DMAC and DEAC with increasing of methanol% or acetone% is dominated by the initial state (IS).

Journal of King Saud University - Science (2015) 27, 54-62,
http://dx.doi.org/10.1016/j.jksus.2014.02.002

$CuFe_2O_4$ nanoparticles: An efficient heterogeneous magnetically Separable catalyst for Synthesis of some novel propynyl-1*H*- imidazoles derivatives

Mahmoud Abd El Aleem Ali Ali El-Remaily and Ahmed M. Abu-Dief
[a]*Department of Chemistry, Faculty of Science, Sohag University- 82524, Sohag, Egypt*
E.mail: msremaily@yahoo.com, msremaily@ugr.es

The non-toxic magnetic $CuFe_2O_4$ nanoparticles have been synthesized, characterized and used as an efficient catalyst for synthesis of new derivatives for 1,2,4,5-tetrasubstituted imidazoles in excellent yields. The synthesized compounds work-up easy and purification of products are performed without chromatographic methods. The catalyst can be recovered for the subsequent reactions and reused without any appreciable loss.

Tetrahedron 71 (2015) 2579e2584, http://dx.doi.org/10.1016/j.tet.2015.02.057

Nano Structure Iron (II) and Copper (II) Schiff Base Complexes of a NNO-Tridentate Ligand as New Antibiotic Agents: Spectral, Thermal Behaviors and DNA Binding Ability

Laila H. Abdel Rahman[a], Ahmed M. Abu-Dief[a], Samer Kamel Hamdan[a] and Amin Abdou Seleem[b]

[a]*Chemistry Department, Faculty of Science, Sohag University, 82534, Egypt*
[b]*Zoology Department, Faculty of Science, Sohag University, 82534 Sohag, Egypt*
laila_kenawy@hotmail.com, ahmed_benzoic@yahoo.com

Complexes of Fe (II) and Cu (II) with a tridentate Schiff base, 2-((z)-(pyridine-2-ylimino) methyl) naphthalene-1-ol derived from 2-hydroxy-1-napthaldehyde and 2-aminopyridine were synthesized. Both the ligand and its complexes were characterized on the basis of microanalysis, melting point, ^{1}H and $^{13}CNMR$, molar conductivity, thermal analysis, IR and UV/Vis spectral studies. From analytical data, the stoichiometry of the complexes was found to be 1: 2 (metal: ligand). The magnetic susceptibilities of all complexes at room temperature were consistent with octahedral geometry. The molar conductance values suggest nonelectrolytes. The IR spectra revealed that the metal ions coordinated through azomethine nitrogen, pyridine nitrogen of and phenolic oxygen of the ligand. The particle size of iron and copper complexes has been investigated by TEM. Antibacterial and antifungal activities in vitro were performed against *three* types of G+ and G- bacteria, *Escherichia coli, Pseudomonas aeruginosa*, *Staphylococcus aureus* and three types of fungi, *Aspergillus flavus, Trichophyton rubrum and Candida albicans* with determination of minimum inhibitory concentrations of ligand and metal complexes. Both complexes showed highly effective antibacterial activities against the tested bacteria and fungi; therefore, these complexes can be used as antibiotic. Furthermore, DNA interaction of Schiff base complexes was monitored by electronic spectra, hydrodynamic measurements and gel electrophoresis. It was found that the prepared complexes could bind to DNA in an intercalating mode.

Int. J. Nano. Chem. 1, No. 2, 65-77 (2015), http://dx.doi.org/10.12785/ijnc/010204

Crystal structure of (E)-1-{[(3,5-dimethylphenyl)imino]methyl}naphthalen-2-ol

Ahmed M. Abu-Dief [a], Mohammed S. M. Abdelbaky[b] and Santiago Garcia-Granda[b]*
[a]*Department of Chemistry, Faculty of Science, Sohag University, 82524 Sohag, Egypt,*
[b]*Department of Physical and Analytical Chemistry, Faculty of Chemistry Oviedo University-CINN, Oviedo 33006, Spain*
sgg@uniovi.es

The title compound, C19H17NO, has an E conformation about the N= C bond. The molecule is relatively planar, with the benzene ring and naphthalene ring plane being inclined to one another by 4.28 (10)°. There is an interamolecular O—H---N hydrogen bond generating an S(6) ring motif. In the crystal, molecules are linked via C—H---O hydrogen bonds, forming chains propagating along [100].Within the chains there are π- π interactions involving the benzene ring and the naphthalene ring system of an adjacent molecule [inter-centroid distance = 3.6405 (14) A°].

Acta Cryst. (2015). E71, 496–497, doi:10.1107/S2056989015011548

Relationship between the Plasma Levels of Leptin, Adiponectin and TNF-Alpha in Diabetic Obesity and Non-Diabetic Obesity in Sohag Governorate, Egypt

Nagwa M. Elsawi[1], Ali Taha A. Hassan[2], Amira M. Ahmed[1], Hossam El-Din M. Omar[3]
[1]*Department of Chemistry, Faculty of Science, Sohage University, Sohage 82524, Egypt*
[2]*Department of Internal Medicine, Faculty of Medicine, Sohag University, Sohag 82524, Egypt*
[3]*Department of Zoology, Faculty of Science, Assiut University, Assiut 71516, Egypt*

Objectives: Obesity is associated with abnormal adipokines production and activation of inflammatory signal pathways in adipose tissue. Also, there is rising facts about the relation between the adiponectin function and pathogenesis of type 2 diabetes. The aim of this study is to investigate the relationship between the levels of leptin, adiponectin, tumor necrosis factor alpha (TNF-α) and lymphocytes count in diabetic and obese diabetic participants and its significance in the etiology of diabetes and obesity in Sohag Governorate.
Methods: 91 unrelated subjects include 34 normal, 49 obese and 8 obese with type 2 diabetes at Hospital of Sohag University were enrolled in this study. Serum leptin, adiponectin and TNF-α levels were measured using ELIZA kit. Fasting and postprandial 2 hours blood glucose level was measured by colorimetric method. Other measurements including blood pressure, BMI and CBR were measured in hospital laboratory.
Results: Both obese and obese diabetic subjects have hyperglycemia and hypertension in comparison with control, however, obese diabetic subjects have higher significant level than obese. Leptin level in serum was significantly higher in obese and obese with type 2 diabetes subjects than control group, where adiponectin level was lower in these subjects than control group. In obese and obese with type 2 diabetes subjects, both of lymphocytes count and level of TNF-α were higher than control and in obese diabetic than obese non diabetic subjects.
Conclusion: The present results showed in obesity with or without type 2 diabetes serum levels of leptin and TNF-α and lymphocytes count were increased, however, adiponectin level was decreased. Moreover, the high level of TNF-α reflect risk factor for vascular diseases like hypertension.

Journal of Diabetes and Obesity. 2(1): 1-4. (2015)
DOI: 10.15436/2376-0494.15.018

In vitro antibacterial activity of *Ipomoea reptans* extracts

Mahmoud H Gad[1], Rehab M Mohamed[3], Nagwa M El-Sawi[2], Sabry H Younes[2], El-Mewafy A El-Ghadban[1]

[1]Department of Medicinal and Aromatic Plants Research, Horticulture Research Institute, Agriculture Research Center, Dokki, Giza, Egypt
[2]Department of Chemistry, Faculty of Science, Sohag University, Sohag, Egypt
[3]Department of Botany, Faculty of Science, Sohag University, Sohag, Egypt

This study was carried out to determine the antibacterial activity of *Ipomoea reptans* extracts which the plant collected from Sudan. All previous literatures and studies carried out but this the first time to study this plant from this area. In this present study, *in vitro* antibacterial activity of nine *Ipomoea reptans* extracts were performed to determine the more active fraction against several Gram-positive and Gram-negative bacterial strains. The results exhibited that hexane (IR1), dichloromethane-ethyl acetate (IR6-1, 6-2 and 7), and ethyl acetate fractions are considered more active whereas dichloromethane-ethyl acetate (IR7, 1:1, v/v) showed more activity against the two tested Gram-positive bacteria (*Bacillus cereus* and *Micrococcus ruseus*). Consequently, five *I. reptans* extracts (IR1, IR61, IR62, IR7 and IR8) demonstrated moderately to highly antibacterial activity against the tested Grampositive bacteria with diameters of inhibition zones ranged from 13 to 17 mm and MIC values ranged from 40 to 120 ppm. Unfortunately, no activity was detected against Gram negative bacteria for all extracts.

Global Advanced Research Journal of Medicine and Medical Science (ISSN: 2315-5159)
Vol. 4(4) pp. 190-193, April, 2015

Biochemical and Histological Studies of Goji Extract Role on Patulin Mycotoxin on Male Rat Kidney

Nagwa M. El-Sawi1[1], Madeha N.Al-Seni[2], Nesreen G. Abd El Haliem[3], Mohamed T. El-Wassimy[1], H. Salah[1], Asma S. Abdo[1]

[1]*Department of Chemistry, Faculty of science, Sohag University, Sohag, Egypt*
[2]*Department of Biochemistry, Faculty of Science, King Abdulaziz University, Jeddah, KSA*
[3]*Department of Histology, Faculty of Medicine, Sohag Univerisity, Sohag, Egypt*

Patulin caused severe damage in several organ systems like kidney, intestinal tissue and immune system. The objective of this study is to show the effects of patulin mycotoxin on some biochemical parameters and histological changes on male rats' kidney. 50 adult albino male rats were divided randomly into 5 groups. Control group was injected subcutaneously daily with distilled water; groups I and II were injected subcutaneously daily with Patulin (0.2 mg/kg/day) for one and two weeks respectively. Group III was treated withthe same dose of patulin for two weeks after that they were injected subcutaneously with Goji extract (2ml/ kg /day) for two weeks. Group IV was treated by Goji for two weeks after that they were treated with the same dose of patulin for two weeks. Level of total antioxidant stress (TAS), Blood urea nitrogen (BUN) and pyruvate kinase (M2-PK) were decreased significantly in serum of both treated groups compared with control group, but level of serum creatinine (SCr), Alpha feto protein (AFP) and carcinoembryonic antigen (CEA) were increased significantly in serum of both treated groups compared with control group. Histopathological changes of rat kidney coincided with biochemical changes. In conclusion, consumption of patulin induced renal toxicity. Goji extract may be used as a new therapeutic for patulin toxicity.

International Journal of Food and Nutritional Science .2(4): 1-7. 2015
DOI: 10.15436/2377-0619.15.036

Protective effect of Lyciumbarbarum extract as Antioxidant Agent on Roridin A Induced Hepatotoxicity in Male Rat

Nagwa M. Elsawi[1], Madeha N. Alseeni[2], Hala I. Madkour[3], Doha S Mohamed[4], Asma. S.Abdo[1]

[1]*Department of Chemistry, Faculty of Science, Sohag University, Sohag, Egypt*
[2]*Department of Biochemistry, Faculty of Science, King Abdel-Aziz University, Jaddah, Saudi Arabia*
[3]*Department of Pharmacology, Faculty of Medicine, Sohag University, Sohag, Egypt*
[4]*Department of Histology, Faculty of Medicine, Sohag University, Sohag, Egypt*

The fruit goji berry of *Lyciumbarbarym*, a traditional Chinese herbal medicine, has been widely used in healthy diets due to its potential role in the prevention of chronic diseases. We studied the effects ofroridin A toxin in male rat liver and their amelioration by goji extract. Thirtymale adult albino rats were divided into three groups (10 rats each). Group 1 (Control group) was given only the solvent(DMSO) of roridin A. Group 2 was administered a single dose (0.6 mg/ kg) of rordin A mycotoxin (dissolved in 1% DMSO) for one week. Group 3 was treated prophylactically with goji extract (5 mg/kg) using gastric tube daily for 6 days and left for one week. Roridin A showed a highly significant increase in serum levels of cholesterol, triglycerides and significant increase inglucose, total antioxidants and tumor necrosis factor (TNF). There was significant decrease in serum ferritin level. On the other hand, administration of goji along with rordin A showed a reduction in the above mentioned factors and elevation inferritin level. Histopathological changes in the rat liver coincided with the above biochemical changes. In conclusion; the treatment of rats with goji extract ameliorated the adverse effects of rordin A. Thus, gojimay be used asan antioxidant for certain toxins.

International Journal of Food and Nutritional Science . 2(3): 1-5.2015
DOI: 10.15436/2377-0619.15.022

Voltammetric Determination of Ferulic Acid Using Polypyrrole Multiwalled Carbon Nanotubes Modified Electrode with Sample Application

Refat Abdel-Hamid and Emad F. Newair
Unit of Electrochemistry Applications (UEA), Chemistry Department, Faculty of Science, Sohag University, Sohag 82524, Egypt

A polypyrrole-multiwalled carbon nanotubes modified glassy carbon electrode-based sensor was devised for determination of ferulic acid (FA). The fabricated sensor was prepared electrochemically using cyclic voltammetry (CV) and characterized using CV and scanning electron microscope (SEM). The electrode shows an excellent electrochemical catalytic activity towards FA oxidation. Under optimal conditions, the anodic peak current correlates linearly to the FA concentration throughout the range of 3.32×10^{-6} to 2.59×10^{-5} M with a detection limit of 1.17×10^{-6} M (S/N= 3). The prepared sensor is highly selective towards ferulic acid without the interference of ascorbic acid. The sensor applicability was tested for total content determination of FA in a commercial popcorn sample and showed a robust functionality.

Nanomaterials, 5 (2015) 1704-1715, DOI:10,3390/nano5041704

Effect of Pretreatment Temperature on the Photocatalytic Activity of Microwave Irradiated Porous Nanocrystalline ZnO

Tarek T. Ali,[ab] Katabathini Narasimharao,[a] Ivan P. Parkin,[c] Claire J. Carmalt,[c] Sanjayan Sathasivam,[c] Sulaiman N. Basahel,[a] Salem M. Bawaked[a], Shaeel A. Al-Thabaiti[a]

[a]Department of Chemistry, Faculty of Science, King Abdulaziz University, P.O. Box 80203, Jeddah 21589, Kingdom of Saudi Arabia. E-mail: ttali@kau.edu.sa

[b]Department of Chemistry, Faculty of Science, Sohag University, P.O. Box 82524, Egypt

[c]Materials Chemistry Centre, Department of Chemistry, University College London, 20 Gordon Street, London WC1H 0AJ, UK

Porous nanocrystalline ZnO photocatalysts were successfully synthesized by microwave irradiation and then thermally treated at different temperatures (150 °C, 200 °C, 250 °C and 300 °C). The physicochemical properties of synthesized samples were determined by using different characterization techniques. The characterization results indicated that the as-synthesized sample was comprised of both ZnO and $Zn(OH)_2$ phases with a particle size of approximately 50 nm. Thermal treatment of the as-synthesized sample at 150 °C resulted in a pure ZnO phase with a particle size of 40 nm. The results also demonstrated that the surface area, pore diameter and bandgap energy reach a maximum value for the ZnO sample treated at 200 °C. The ZnO nanoparticles pretreated at 200 °C showed the highest photocatalytic activity (99% of degradation) in a short reaction time (90 min), which can be attributed to the combined effects of several factors including low crystallite size, relatively high surface area, pore diameter, pore volume and bandgap energy. Reusability results show that the catalysts can be readily separated from the reaction mixture by filtration after the photocatalytic reaction and reused at least five times without any loss of activity.

New Journal of Chemistry, 39 (2015) 321 – 332, DOI: 10.1039/c4nj01465k

Influence of Crystal Structure of Nanosized ZrO_2 on Photocatalytic Degradation of Methyl Orange

Sulaiman N Basahel[1], Tarek T Ali[1,2], Mohamed Mokhtar[1,3], Katabathini Narasimharao[1]
[1]Department of Chemistry, Faculty of Science, King Abdulaziz University, 80203, Jeddah 21589, Kingdom of Saudi Arabia.
[2]Chemistry Department, Faculty of Science, Sohag University, 82524, Sohag 82524, Egypt
[3]Physical Chemistry Department, National Research Centre, El Buhouth St., Dokki, Cairo 12622, Egypt

Nanosized ZrO_2 powders with near pure monoclinic, tetragonal, and cubic structures synthesized by various methods were used as catalysts for photocatalytic degradation of methyl orange. The structural and textural properties of the samples were analyzed by X-ray diffraction, Raman spectroscopy, TEM, UV-vis, X-ray photoelectron spectroscopy (XPS), and N2 adsorption measurements. The performance of synthesized ZrO_2 nanoparticles in the photocatalytic degradation of methyl orange under UV light irradiation was evaluated. The photocatalytic activity of the pure monoclinic ZrO_2 sample is higher than that of the tetragonal and cubic ZrO_2 samples under optimum identical conditions. The characterization results revealed that monoclinic ZrO_2 nanoparticles possessed high crystallinity and mesopores with diameter of 100 Å. The higher activity of the monoclinic ZrO_2 sample for the photocatalytic degradation of methyl orange can be attributed to the combining effects of factors including the presence of small amount of oxygen-deficient zirconium oxide phase, high crystallinity, large pores, and high density of surface hydroxyl groups.

Nanoscale Research Letters, 10:73 (2015) 2 – 13, DOI: 10.1186/s11671-015-0780-z

Degradation and mineralization of organic UV absorber compound 2-Phenylbenzimidazole-5-sulfonic acid (PBSA) using UV-254 nm/H_2O_2

Wael H. M. Abdelraheem[1, 2], Xuexiang He[2, 3], Xiaodi Duan[2, 3], Dionysios D. Dionysiou[2, 3]

[1]*Chemistry Department, Faculty of Science, Sohag University, Sohag 82524, Egypt*

[2]*Environmental Engineering and Science Program, University of Cincinnati, Cincinnati, Ohio 45221-0012, United States*

[3]*NIREAS-International Water Research Center, University of Cyprus, Nicosia, 1678, Cyprus*

dionysios.d.dionysiou@uc.edu

Various studies have revealed the non-biodegradable and endocrine disrupting properties of sulfonated organic UV absorbers, directing people's attention towards their risks on ecological and human health and hence their removal from water. In this study, UV-254 nm/H_2O_2 advanced oxidation process (AOP) was investigated for degrading a model UV absorber compound 2-Phenylbenzimidazole-5-sulfonic acid (PBSA) and a structurally similar compound *1H*-Benzimidazole-2-sulfonic acid (BSA), with a specific focus on their mineralization. At 4.0 mM $[H_2O_2]_o$, a complete removal of 40.0 µM parent PBSA and 25% decrease in TOC were achieved with 190 min of UV irradiation; SO_4^{2-} was formed and reached its maximum level while the release of nitrogen as NH_4^+ was much lower (around 50%) at 190 min. Sulfate removal was strongly enhanced by increasing $[H_2O_2]_o$ in the range of 0-4.0 mM, with slight inhibition in 4.0-12.0 mM. Faster and earlier ammonia formation was observed at higher $[H_2O_2]_o$. The presence of Br^- slowed down the degradation and mineralization of both compounds while a negligible effect on the degradation was observed in the presence of Cl^-. Our study provides important technical and fundamental results on the $HO^\bullet$ based degradation and mineralization of $-SO_3H$ and N-containing UV absorber compounds.

Journal of Hazardous Materials, 282, 2015, 233-240,
DOI:10.1016/j.jhazmat.2014.07.041

Multicomponent green synthesis, spectroscopic and structural investigation of multi-substituted imidazoles

Shaaban K. Mohamed[1] / Jim Simpson[2] / Adel A. Marzouk[3] / Avtandil H. Talybov[4] / Antar A. Abdelhamid[5] / Yusif A. Abdullayev[4]/ Vagif M. Abbasov[4]

[1]Chemistry and Environmental Division, Manchester Metropolitan University, Manchester, M1 5GD, England ,[2]Department of Chemistry, University of Otago, P. O. Box 56, Dunedin, New Zealand, [3]Faculty of Pharmacy, Pharmaceutical Chemistry Department, Al Azhar University, Egypt, [4]Mamedaliev Institute of Petrochemical Processes, National Academy of Sciences of Azerbaijan, Baku, Azerbaijan, [5]Faculty of Science, Department of Chemistry, Sohag University, 82524 Sohag, Egypt

drantar25@yahoo.com

Ten 1,2,4,5-tetra-substituted imidazole derivatives have been synthesized with a 2-hydroxyethy substituent at the 1-nitrogen atom and potentially electron releasing hydroxy-, methoxy-, dimethylamino- or nitro substituents in various positions on the benzene ring located on the 2-carbon atom. The prototypical derivative with an unsubstituted phenyl ring at the 2-position is also reported. The compounds are obtained in excellent yields (average 86%) via a four-component cyclocondensation reaction of benzil, ethanolamine, and the appropriate aromatic carbaldehyde together with ammonium acetate. The reaction uses a novel ionic liquid catalyst, DEAHS (diethyl ammonium hydrogen sulfate), under solvent-free conditions and a green synthetic protocol. The key advantages of this process are high yield, shorter reaction times and ease of work-up. Furthermore, the products can be purified by a non-chromatographic method and the catalyst is re-usable. All of these newly synthesized compounds have been characterized from spectral data; the X-ray structures of three representative molecules are also detailed.

Zeitschrift für Naturforschung B. 70 (2015)809–817, DOI: 10.1515/znb-2015-0067

Synthesis and Anti-inflammatory Study of Novel N-substituted Hydroacridine-1,8-diones and Bis-hexahydroacridine-1,8-dione Derivatives

Omyma A Abd-Allah[1], Antar A Abdelhamid[1] and Shaaban K Mohamed[2]
[1]Department of Chemistry, Faculty of Science, Sohag University, Sohag, Egypt
[2]Chemistry and Environmental Division, Manchester Metropolitan University, Manchester M1 5GD, England
drantar25@yahoo.com

We report in this study the synthesis of some new N-substituted hexahydro- acridine-1,8-dione compounds including some new N- 2-hydroxypropylhexahydro- acridine-1,8-diones and their tosylatedoctahydroacridine-1,8-dione derivatives in addition to some bis-hexahydroacridine-1,8-diones via a one pot reaction technique. Moreover, in vivo anti-inflammatory evaluation for some newly synthesized compounds has been investigated. The highly alkylated bishydroacridine-1,8-dione 5f showed a higher anti- inflammatory potency more than the non-alkylated and the standard employed indomethacin. The structure of all new products has been characterized by IR, ^{1}H-NMR and ^{13}C-NMR.

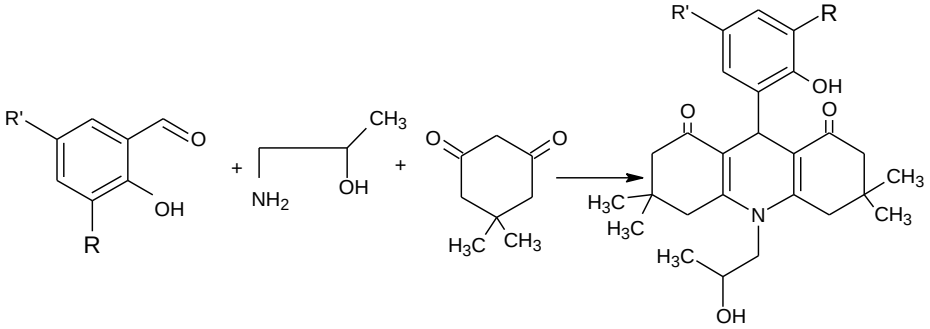

Compound 2 R= Br, R'= Cl
Compound 3 R= H, R'= H

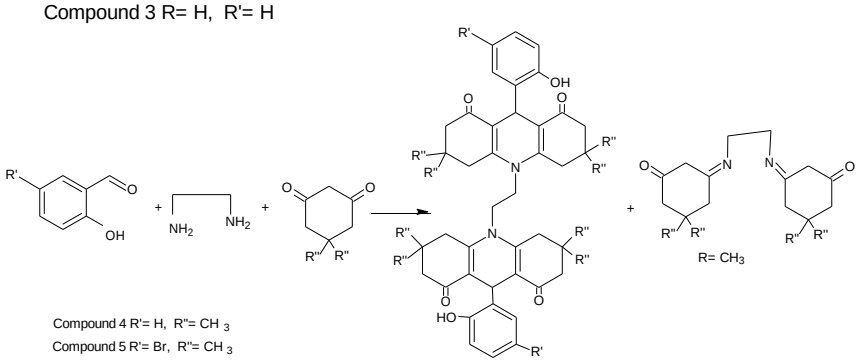

Compound 4 R'= H, R''= CH_3
Compound 5 R'= Br, R''= CH_3
Compound 10 R'= H, R''= H
Compound 11 R'= Br, R''= H
Compound 5 R'= Br, R''= CH_3

Med chem (2015) S 2, 2161-0444.10000, DOI: 10.4172/2161-0444.1000004

Electrochemistry with the extremely weak coordinating anions: Using of carboranes $[H\text{-}CB_{11}X_6Y_5]^-$ (X = H, Cl, Br; Y = H or Me) as supporting electrolyte anions

Ayman Nafady

Department of Chemistry, College of Science, King Saud University, Riyadh, Saudi Arabia
Department of Chemistry, Faculty of Science, Sohag University, Sohag, Egypt

This work demonstrates the feasibility of utilizing arguably the most inert, least basic, and extremely weak coordinating carborane anions, $[H\text{-}CB_{11}X_6Y_5]^-$ (X=H, Cl, Br; Y=H orMe), as supporting electrolytes in low-polarity media. The redox behaviors of somemodel systems such as ferrocene (Fc), $CoCp(CO)_2$ and $[(\eta6\text{-}C6Me_6)RhCp]^{2+}$ in the presence of $[NBu_4][H\text{-}CB_{11}H_{11}]$, $[NBu_4][H\text{-}CB_{11}Cl_6Me_5]$ and $[NBu_4][H\text{-}CB_{11}Br_6Me_5]$ resemble those observed with other weakly coordinating anions (WCAs) such as $[B(C_6F_5)_4]^-$ and $[Al(OC(CF_3)_3)_4]^-$. The overall results show that this class of carborane anions is a promising candidate for a new generation of WCA-based supporting electrolytes, for exploration the molecular electrochemistry of various organic, inorganic and organometallic compounds.

Journal of Electroanalytical Chemistry 755 (2015) 1-6,
DOI:.org/10.1016/j.jelechem.2015.07.028

Glycine-assisted synthesis of NiO hollow cage-like nanostructures for sensitive non-enzymatic glucose sensing

Zafar Hussain Ibupoto, Aynam Nafady, Razium Ali Soomro, Sirajuddin, Syed TufailHussain Sherazi, Muhammad Ishaq Abroe and Magnus Willander
[a]*Institute of Chemistry University of Sindh Jamshoro, 76080, Pakistan*
[b]*Department of Chemistry, Sohag University, Cairo, 8252, Egypt*
raziumsoomro@gmail.com

In this work, a highly sensitive non-enzymatic glucose sensor was developed based on NiO hollow cage-like nanostructures (NiO HCs). The novel nanostructures were synthesized using hydrothermal growth route with glycine employed as an effecient growth director. The synthesized NiO HCs were characterized by using scanning electron microscopy (SEM), X-ray photoelectron microscopy (XPS) X-ray diffraction (XRD) and Fourier transform infrared (FTIR) techniques for morphological, compositional and structural determination respectively. The prepared NiO HCs were directly integrated to be structured electrodes exhibiting enhanced electrocatalytic performance toward the oxidation of glucose with high sensitivity (2476.4 mA mM1 cm2), low detection limit (LOD) (0.1 mM), wide detection range (0.1–5.0 mM) (r2 ¼ 0.9997) and excellent reproducibility. The developed nonenzymatic glucose sensor further demonstrated excellent anti-interference property in the presence of common interferents such as uric acid (UA), dopamine (DP) and ascorbic acid (AS). The role of glycine molecules as an efficient growth directing agent with a plausible growth mechanism has also been highlighted. In addition, the NiO HCs modified electrode was also used to analyze glucose concentration in human serum samples. The excellent sensing performance can be attributed to the unique morphology, which allowed increased electron transfer passages with lower charge transfer resistance, and enhanced molecular approach during electrochemical sensing offered from nanoscale ―hollow cage‖ units of NiO structures

RSC Adv.,2015,5, 18773, DOI: 10.1039/c4ra15858j

Catalytic Reductive Degradation of Methyl Orange Using Air Resilient Copper Nanostructures

Razium Ali Soomro, Nazar Hussain Kalwar, Ayman Nafady, Sirajuddin, Mohammad Raza Shah, Syed Tufail Hussain Sherazi, and Keith Richard Hallam

National Centre of Excellence in Analytical Chemistry, University of Sindh, Jamshoro 76080, Pakistan

Interface Analysis Centre, School of Physics, University of Bristol, Bristol BS8 1TL, UK

Department of Chemistry, College of Science, King Saud University, Riyadh 11451, Saudi Arabia

Chemistry Department, Faculty of Science, Sohag University, Sohag 82524, Egypt

International Centre for Chemical and Biological Sciences, H.E.J. Research Institute of Chemistry University of Karachi, Karachi 75500, Pakistan, nazarkalwar@gmail.com

The study describes the application of oxidation resistant copper nanostructures as an efficient heterogeneous catalyst for the treatment of organic dye containing waste waters. Copper nanostructures were synthesized in an aqueous environment using modified surfactant assisted chemical reduction route. The synthesized nanostructures have been characterized by UV-Vis, Fourier transform infrared spectroscopy FTIR spectroscopy, Atomic force microscopy (AFM), Scanning Electron Microscopy (SEM), and X-ray diffractometry (XRD). These surfactant capped Cu nanostructures have been used as a heterogeneous catalyst for the comparative reductive degradation of methyl orange (MO) in the presence of sodium borohydride (NaBH)usedasapotential reductant. Copper nanoparticles (Cu NPs) were found to be more efficient compared to copper nanorods (Cu NRds) with the degradation reaction obeying pseudofirst order reaction kinetics. Shape dependent catalytic efficiency was further evaluated from activation energy of reductive degradation reaction. The more efficient Cu NPs were further employed for reductive degradation of real waste water samples containing dyes collected from the drain of different local textile industries situated in Hyderabad region

Hindawi Publishing Corporation, Journal of Nanomaterials, 2015,1-12, 2015

Tranexamic acid derived gold nanoparticles modified glassy carbonelectrode as sensitive sensor for determination of nalbuphine

Tayyaba Shaikh, Ayman Nafady, Farah N. Talpur, Sirajuddina, Muhammad H. Agheemd, Muhammad R. Shahe, Syed Tufail H. Sherazia,Razium A. Soomroa, Samia Siddiqui

National Center of Excellence in Analytical Chemistry, University of Sindh, A-333, Phase 1, SUECHS, Jamshoro 76080, PakistanbDepartment of Chemistry, College of Science, King Saud University, Riyadh, Saudi ArabiacChemistry Department, Faculty of Science, Sohag University, Sohag 82524, Egypt, drsiraj03@yahoo.com

We display a simple chemical procedure for fabrication of spherical gold nanoparticles (AuNps) usingtranexamic acid (Tr) as reducing as well as capping agent. As-formed Tr-AuNps were characterized byUltra Violet Visible (UV–Vis) spectroscopy where the surface plasmon absorption band was controlledat 522 nm under already optimized conditions. Atomic force microscopy (AFM) unveiled informationin relation to size and shape of Tr-AuNps. Fourier transform infra red (FTIR) spectroscopy divulged theinteraction between capping agent and AuNps while X-ray diffractometry (XRD) disclosed the natureof crystalline patterns of AuNps. As-prepared Tr-AuNps were sandwiched between the surface of glassycarbon electrode (GCE) and nafion and used as sensor for highly selective and sensitive voltammetricdetermination of nalbuphine (NA) using square wave voltammetry (SWV) as analytical mode. Param-eters such as volume of nafion, working electrodes, type and ionic strength of supporting electrolyte,pH, stirring rate, initial potential, accumulation potential and accumulation time were optimized. Themechanism regarding the oxidation of NA was also proposed. The sensor responded linearly in the rangeof 0.05–1.25 g mL^{-1} NA with excellent limit of detection (LOD) of 13.2 ng mL-1and R2value of 0.997. Inaddition, the sensor performed linearly to NA even within the matrices of serum as well as urine samples.The fabricated sensor demonstrated higher selectivity for sensitive determination of NA in the presenceof various interfering species commonly found in human serum and urine. The developed sensor wassuccessfully applied and validated for the determination of NA in human serum and urine samples withexcellent recoveries.

Sensors and Actuators B 211 (2015) 359–369, Doi: org/10.1016/j.snb.2015.01.096

Development of sensitive non-enzymatic glucose sensor using complex nanostructures of cobalt oxide

Razium Ali Soomro, Aynam Nafady , Zafar Hussain Ibupoto, Syed Tufail Hussain Sherazi, Magnus Willander, Sirajuddin, Muhammad Ishaq Abro

Department of Science and Technology, Campus Norrkoping, Linkoping University, SE-60174 Norrkoping, Sweden

Department of Metallurgy and Materials Engineering, Mehran University of Engineering and Technology, Jamshoro 76080, Pakistan

Department of Chemistry, Faculty of Science, Sohag University, Sohag, Egypt

raziumsoomro@gmail.com

The study reports the synthesis of cobalt oxide (Co_3O_4) nanostructures and their application in enzyme free electrochemical sensing of glucose. The synthesized nanostructures were elaborately characterized via number of analytical techniques including scanning electron microscopy, X-ray diffraction (XRD), X-ray photoelectron spectroscopy (XPS) and Fourier transform infrared spectroscopy (FTIR). The as-synthesized nanostructures of Co_3O_4 were found to exhibited nanodisc like morphology with the size dimension in range of 300–500 nm. The obtained morphological features were evaluated for their electrochemical potential towards oxidation of glucose which enabled development of sensitive (27.33 $mAmM^{-1}$ Cm^{-2}), and stable enzyme free glucose sensor. In addition, the developed sensor showed excellent linearity (r 2 ¼0.9995), wide detection range (0.5– 5.0 mM), lower detection limit (0.8 mM) and extreme selectivity towards glucose in the presence of common interferents like dopamine (DP), ascorbic acid (AA) and uric acid (UA). The successfully application of developed sensor for real blood glucose analysis further reflects its capability for routine glucose measurement.

Materials ScienceinSemiconductorProcessing34(2015)373-381,